Development 137, 3835-3845 (2010) doi:10.1242/dev.055483

The transcription factor grainyhead-like 2 regulates the molecular composition of the epithelial apical junctional complex

Max Werth[1,2,*], Katharina Walentin[1,2,*], Annekatrin Aue[1,2], Jörg Schönheit[1], Anne Wuebken[1], Naomi Pode-Shakked[3], Larissa Vilianovitch[1], Bettina Erdmann[1], Benjamin Dekel[3], Michael Bader[1], Jonathan Barasch[4], Frank Rosenbauer[1], Friedrich C. Luft[1,2] and Kai M. Schmidt-Ott[1,2,†]

SUMMARY

Differentiation of epithelial cells and morphogenesis of epithelial tubes or layers is closely linked with the establishment and remodeling of the apical junctional complex, which includes adherens junctions and tight junctions. Little is known about the transcriptional control of apical junctional complex components. Here, we show that the transcription factor grainyhead-like 2 (Grhl2), an epithelium-specific mammalian homolog of *Drosophila* Grainyhead, is essential for adequate expression of the adherens junction gene E-cadherin and the tight junction gene claudin 4 (*Cldn4*) in several types of epithelia, including gut endoderm, surface ectoderm and otic epithelium. We have generated *Grhl2* mutant mice to demonstrate defective molecular composition of the apical junctional complex in these compartments that coincides with the occurrence of anterior and posterior neural tube defects. Mechanistically, we show that Grhl2 specifically associates with cis-regulatory elements localized at the Cldn4 core promoter and within intron 2 of the E-cadherin gene. Cldn4 promoter activity in epithelial cells is crucially dependent on the availability of Grhl2 and on the integrity of the Grhl2-associated cis-regulatory element. At the E-cadherin locus, the intronic Grhl2-associated cis-regulatory region contacts the promoter via chromatin looping, while loss of Grhl2 leads to a specific decrease of activating histone marks at the E-cadherin promoter. Together, our data provide evidence that Grhl2 acts as a target gene-associated transcriptional activator of apical junctional complex components and, thereby, crucially participates in epithelial differentiation.

KEY WORDS: Apical junctional complex, E-cadherin (*Cdh1*) gene regulation, Epithelial differentiation, Grainyhead transcription factors, Grainyhead-like 2 (*Grhl2*), Claudin 4 (*Cldn4*), Neural tube defects, Mouse

INTRODUCTION

Epithelial cells structurally compartmentalize multi-cellular organisms. Differentiation of epithelial cells during development is closely associated with the formation of an apical junctional complex, a multifunctional membrane-associated apparatus, which is required for the establishment of epithelial polarity and for the acquisition and maintenance of epithelial-specific functions (Halbleib and Nelson, 2006; Meng and Takeichi, 2009; Tepass, 2003; Wang and Margolis, 2007). Two structural hallmarks of the apical junctional complex are adherens junctions and tight junctions. Adherens junctions mediate stable adhesion between epithelial cells and play a central role in initial cell sorting (Halbleib and Nelson, 2006; Meng and Takeichi, 2009). Tight junctions regulate paracellular permeability for water and solutes (Tepass, 2003). In addition, both tight junctions and adherens junctions participate in the establishment of apico-basal polarity and the regulation of signal transduction (Wang and Margolis, 2007). The central molecular components of adherens junctions include the cadherins, homophilic cell adhesion molecules that participate in both structural properties of the adherens junction and in signal transduction (Halbleib and Nelson, 2006; Meng and Takeichi, 2009; Vleminckx and Kemler, 1999). Cell-cell contacts at the tight junction are intimately linked to proteins of the claudin family (Tepass, 2003). Overall, the molecular composition of the apical junctional complex determines the mechanical stability of cell-cell adhesion between adjacent epithelial cells, the permeability of the epithelial layer for solutes, and cell type-specific signal transduction.

E-cadherin is a signature member of the cadherin family and constitutes a key component of adherens junctions (Gumbiner, 2005). E-cadherin mutant mouse embryos fail to develop beyond the blastocyst stage and fail to form organized tissues, illustrating the importance of this molecule in development (Larue et al., 1996). Furthermore, E-cadherin is a key suppressor of invasion and metastasis in cancer and its downregulation has been linked to the progression of neoplasms (Behrens et al., 1989; Halbleib and Nelson, 2006). E-cadherin transcription is highly modulated during cell type transitions in the embryo. For example, during gastrulation E-cadherin is decreased in delaminating epiblast cells that undergo epithelial-to-mesenchymal transition. Conversely, E-cadherin transcription is re-induced in mesenchymal cells that undergo epithelial conversion during kidney development. Remarkably, in this context, the induction of E-cadherin is temporally coordinated with the expression of multiple additional

[1]Max-Delbrück Center for Molecular Medicine, Robert-Rössle-Strasse 10, 13125 Berlin, Germany. [2]Experimental and Clinical Research Center, Charité-Universitätsmedizin Berlin, Campus Buch, 13125 Berlin, Germany. [3]Department of Pediatrics and Pediatric Stem Cell Research Institute, Sheba Medical Center, Tel Hashomer, 52621, Israel. [4]Department of Medicine, Columbia University College of Physicians and Surgeons, New York, NY 10032, USA.

*These authors contributed equally to this work
†Author for correspondence (kai.schmidt-ott@mdc-berlin.de)

Accepted 14 September 2010

components of the apical junctional complex, suggesting that a common molecular mechanism orchestrates the induction of apical junctional complex components during epithelial differentiation (Schedl, 2007; Schmidt-Ott et al., 2007).

The transcriptional regulation of apical junctional complex components, including E-cadherin, is incompletely understood. Several transcriptional repressors of E-cadherin have been identified, which bind to the promoter region and include the zinc-finger transcription factors Slug, Snail, Zeb1 and Zeb2, and the basic helix-loop-helix transcription factors Twist and E12/E47 (Batlle et al., 2000; Cano et al., 2000; Carver et al., 2001; Comijn et al., 2001; Conacci-Sorrell et al., 2003; Grooteclaes and Frisch, 2000; Peinado et al., 2004; Perez-Moreno et al., 2001; Yang et al., 2004). However, the E-cadherin promoter is insufficient to drive E-cadherin-specific reporter expression in mice (Stemmler et al., 2003). Hence, additional cis-regulatory elements must exist that ensure epithelial-specific expression of E-cadherin. Such elements have been localized downstream of the transcriptional start site (TSS). When sequences from +0.1 to +11 kb from the TSS of the E-cadherin gene are combined with the core promoter in transgenic reporter assays, epithelial-specific enhancer activity is observed in endodermal and ectodermal epithelia (Stemmler et al., 2003). In addition, upon deletion of intron 2 in mice, the E-cadherin locus becomes inactive during early embryonic development and assumes only weak activity after day E11.5 of embryonic development (Stemmler et al., 2005). These data indicate that intron 2 contains both necessary and sufficient regulatory elements for epithelium-specific E-cadherin expression, and suggest that unknown transcriptional activators associate with this cis-regulatory region to facilitate cell type-specific E-cadherin transcription.

In this study, we show that Grhl2, a mammalian homolog of *Drosophila* Grainyhead, regulates epithelial differentiation and determines expression levels of E-cadherin and claudin 4 (Cldn4). Mechanistically, we show that Grhl2 associates with conserved cis-regulatory elements at the Cldn4 promoter and in intron 2 of E-cadherin, and comprises an essential component of the transcriptional machinery that establishes appropriate expression levels of these genes in different types of epithelia.

MATERIALS AND METHODS

Animals

The two Grhl2-deficient alleles Grhl2^{LacZ1} and Grhl2^{LacZ4} were derived from distinct embryonic stem (ES) cell clones containing gene traps of the Grhl2 locus: clone E115B04 (German Gene Trap Consortium, Munich, Germany) and clone RRU622 (BayGenomics, San Francisco, CA), respectively (see Fig. S1 in the supplementary material). The gene trap vector integration site of clone E115B04 had been determined by the distributor, whereas the integration site of clone RRU622 was determined by Splinkerette PCR (Horn et al., 2007) using primers detailed in Table S1 in the supplementary material. ES cells were injected into C57BL/6 recipient blastocysts (16-18 cells per blastocyst) and subsequently transferred into C57BL/6 foster mice. All mice used in this study have a mixed 129P2/C57BL/6 (E115B04, Grhl2^{LacZ1}) or 129/ola/C57BL/6 (RRU622, Grhl2^{LacZ4}) genetic background. Mice were genotyped via PCR using primers indicated in Table S1 in the supplementary material.

Cell culture

Mouse inner medullary collecting duct (mIMCD-3) cells were purchased from ATCC (CRL-2123) and transfected using FuGene transfection reagent (Roche Applied Science, Mannheim, Germany). For establishment of stably transfected cells, G418 selection was performed for 2 weeks, and individual clones were subsequently expanded and analyzed.

Human tissue samples

Human adult kidney, renal cell carcinoma and Wilms tumor surgical samples were retrieved from patients within an hour of surgery. Human fetal kidney samples were collected from elective abortions (fetal age 14-19 weeks). All studies were approved by the local ethical committees of Sheba and Asaf Harofeh Medical Center, Hadassah-Ein Kerem and Wolfson hospital in Israel. Informed consents were provided by the legal guardians of the patients or by the patients themselves, according to the declaration of Helsinki.

Antibodies

The following antibodies were used: anti-Grhl2 (HPA004820, Sigma-Aldrich, Munich, Germany), anti-Foxa2 (ab40874, Abcam, Cambridge, UK), anti-Pax2 (716000, Invitrogen, Karlsruhe, Germany), anti-β-catenin (610154, BD Biosciences, Heidelberg, Germany), anti-E-cadherin (610182, BD Biosciences), anti-N-cadherin (610920, BD Biosciences), anti-Tjp1 (412200, Invitrogen), anti-occludin (ab31721, Abcam), anti-mouse-HRP (A2554, Sigma), anti-rabbit-HRP (A0545, Sigma), anti-acetyl-histone-H3-K9/14 (06-599, Millipore, Billerica, MA), anti-trimethyl-histone-H3-K4 (ab8580, Abcam), anti-Aqp1 (AB3065, Millipore), rabbit anti-Nkcc2 (a gift from Sebastian Bachmann, Charité Berlin), rabbit anti-Ncc (a gift from David Ellison, Oregon Health and Science University), anti-Aqp2 (ab15116, Abcam) and anti-β-galactosidase (ab9361, Abcam).

Plasmids

shRNA hairpins were cloned into pSuper.retro.neo+gfp vector (Oligoengine, Seattle, WA) according to manufacturer's instructions. Grhl2-shRNA1 targets the sequence 5′-TCAACAAAGGACAATTCTA-3′, Grhl2-shRNA2 targets the sequence 5′-GACTTCCCCTGATGATTCA-3′. An empty shRNA vector was used as a negative control in luciferase reporter assays. In all other experiments, an shRNA targeting the sequence 5′-CATCACGTACGCGGAATACT-3′ of firefly luciferase was used as a negative control. Full-length mouse Grhl2 was amplified by PCR and subcloned into pCi-neo (Promega). Silent mutations were induced to yield the expressed mRNA resistant to Grhl2-shRNA2 using Quick-Change Mutagenesis Kit (Stratagene, La Jolla, CA). To construct a GFP-labeled dominant-negative mutant of Grhl2, a truncated version of Grhl2 (lacking amino acids 1-232) was cloned into pEGFP-C2 vector (Clontech, Saint-Germain-en-Laye, France). The Cldn4 reporter construct was generated by inserting bases –611 to +174 relative to the Cldn4 TSS into pGL3-Basic vector (Promega). Deletion constructs and mutagenized constructs were generated as indicated using Quick-Change Kit (Stratagene).

Immunofluorescence staining, *lacZ* staining and in situ hybridization

Embryos or adult kidney blocks were fixed in PBS/4% paraformaldehyde, cryosectioned and subjected to immunofluorescence staining using blocking buffer (PBS/0.2% bovine serum albumin/0.05% Triton X-100), primary antibodies as indicated and secondary antibodies labeled by Cy2, Cy3 or Cy5 (Jackson ImmunoResearch, Newmarket, UK). Nuclei were visualized using SYTOX green or TO-PRO-3 (Invitrogen). Imaging was performed on an inverted TCS SP5 Tandem confocal microscope (Leica Microsystems GmbH, Wetzlar, Germany). Whenever relative intensity of immunofluorescent staining was compared, the *z*-plane was adjusted for maximal fluorescence intensity and image acquisition settings were maintained identical for all samples. LacZ staining was carried out as described previously (Zhang et al., 2009). Whole-mount or section in situ hybridization on embryos or kidneys was carried out as described previously (Hammes et al., 2001; Schmidt-Ott et al., 2007). Riboprobes for E-cadherin and Cldn4 were produced from PCR fragments (see Table S1 in the supplementary material). The Grhl2 riboprobe was produced from a 1.9 kb Grhl2 cDNA fragment inserted into pCI-neo. Digoxigenin-labeled cRNA was produced using T7 polymerase or T3 polymerase as appropriate.

Electron microscopy

E9.5 embryos were fixed with 3% glutaraldehyde in 0.1 M cacodylate buffer and 2 mM $CaCl_2$ for 24 hours, and postfixed with 1% OsO_4 and 0.8% $K_3Fe(CN)_6$ in 0.1 M cacodylate buffer for 2 hours. Following en bloc

staining with 4% uranyl acetate, the samples were dehydrated in a graded ethanol series and propylene oxide and embedded in Poly/Bed 812 (Polysciences, Eppelheim, Germany). Ultrathin sections (70 nm) were contrasted with uranyl acetate and lead citrate, and examined with a Zeiss 910 electron microscope. Digital images were taken with a 1kx1k high-speed slow scan CCD camera (Proscan).

SDS PAGE and western blotting

Whole-cell lysates were prepared using RIPA buffer (50 mM Tris-HCl, 150 mM NaCl, 1% IGEPAL, 0.5% sodium deoxycholate, 0.1% SDS, protease inhibitors cocktail). SDS-PAGE was performed using Novex Bis-Tris 4-12% precast gels (Invitrogen) according to the manufacturer's instructions. After electrophoresis, proteins were transferred onto PVDF membrane using 48 mM Tris, 39 mM glycine buffer (pH=9.2).

RNA extraction and cDNA synthesis

Total RNA was isolated using RNeasy Mini Kit (Qiagen, Hilden, Germany) according to the manufacturer's instructions including treatment with RNase-free DNase I (Qiagen). First-strand cDNA synthesis was carried out from 100 ng of total RNA from each sample with the RevertAid First Strand cDNA Synthesis Kit (Fermentas GmbH, St. Leon-Rot, Germany), according to the manufacturer's instructions.

Real-time PCR

Real-time PCR was performed using DNA or cDNA as a template and MESA GREEN qPCR MasterMix Plus for SYBR Assay Rox (Eurogentec, Cologne, Germany). Primer sequences are listed in Table S1 in the supplementary material. Relative levels of mRNA expression were normalized for β-actin mRNA expression (for real-time RT-PCR) or for total input (for ChIP experiments), and calculated according to the ΔΔCT method as previously described (Schmidt-Ott et al., 2007).

Microarray analysis

Affymetrix Mouse Genome 430 2.0 microarrays from mouse E12.5 ureteric bud tips, ureteric bus stalks and metanephric mesenchymes have been published previously and are deposited in Gene Expression Omnibus (GEO) (Schmidt-Ott et al., 2005). We added a new microarray analysis from a subclone of mIMCD-3 cells representing epithelial cells on the same microarray platform (Affymetrix, Santa Clara, CA) and recalculated expression values in the complete dataset by robust multichip analysis as previously described (Schmidt-Ott et al., 2005). We identified genes with significant differential expression using *t*-test on the GEPAS platform (Herrero et al., 2003). The epithelial signature genes and transcription factors presented here displayed at least sixfold overexpression in epithelial samples at a $P<0.05$. Results have been deposited in Gene Expression Omnibus (GEO) with Accession Number GSE24295.

Chromatin immunoprecipitation assay

mIMCD-3 cells were grown to 100% confluence, 5×10^6 cells were cross-linked with 1% formaldehyde for 20 min at room temperature. Chromatin was fragmented to an average size of 300-500 bp. Chromatin (100 μg) and 5 μg of antibody was used per assay using Chromatin Immunoprecipitation Kit (Upstate).

Reporter assays

Reporter assays were performed as described previously (Schmidt-Ott et al., 2007) using firefly luciferase reporter vectors and a Renilla luciferase plasmid for normalization. Cells were harvested after 24 hours of culture and reporter activity was assayed using the Dual Luciferase Assay System (Promega, Madison, WI).

Chromatin conformation capture (3C)

We employed the Chromosome Conformation Capture (3C) procedure (Dekker et al., 2002) with minor modifications. Briefly, mIMCD-3 cell extracts were prepared from 10^7 cells by crosslinking with 2% formaldehyde for 10 minutes at 4°C followed by quenching with 0.125 M glycine. Cell lysates were prepared in 10 mM Tris (pH 8.0), 10 mM NaCl and 0.2% NP40 including proteinase inhibitors, and nuclei were resuspended in NEBuffer 3, lysed by adding SDS to a final concentration of 0.3% and incubating at 37°C for 1 hour. Triton X-100 was added to a final concentration of 1.8% followed by incubation at 37°C for 1 hour. Subsequently, crosslinked nuclear extracts were digested with 800 U of *Bgl*II (New England Biolabs) for 16 hours followed by restriction enzyme inactivation using SDS at a final concentration of 1.5% and incubation at 65°C for 20 minutes. Fifteen percent of the crosslinked and digested extracts was diluted in a total volume of 4 ml and ligated at 16°C for 16 hours using 40,000 U of T4 ligase (New England Biolabs) and the appropriate buffer. Religated products were digested with proteinase K at 65°C for 16 hours followed by phenol/chloroform extraction and ethanol precipitation. Religation was tested by PCR using primers indicated in Table S1 in the supplementary material.

Statistical analysis

Statistical significance of differences between two groups was analyzed using two-sided Student's *t*-test. If more than two groups were compared, two-way ANOVA with post-hoc Tukey or Dunnett test was used.

RESULTS

Grhl2 is co-regulated with E-cadherin across different types of mammalian epithelia

In an effort to identify transcription factors co-regulated with the signature apical junctional complex gene E-cadherin we analyzed gene expression in epithelial and non-epithelial cell types using microarrays. We analyzed an epithelial cell line (mIMCD-3) and the early embryonic kidney, which allows a compartmental separation of epithelial (ureteric bud) and non-epithelial (metanephric mesenchyme) cells (see Fig. S2A in the supplementary material) (Schedl, 2007; Schmidt-Ott et al., 2005). As predicted, genes overexpressed in epithelial cells (when compared with non-epithelial cells) included components of the apical junctional complex (adherens junction, tight junction, desmosomes, apical polarity complex) and the epithelial cytoskeleton (see Fig. S2B in the supplementary material). We obtained functional annotations for all epithelial-specific genes using gene ontology databases and the published literature to identify epithelial-specific transcription factors (see Fig. S2C in the supplementary material). In addition, we calculated correlation coefficients of expression levels between all known transcription factors represented on the microarray and E-cadherin, revealing that five transcription factors displayed a near-perfect correlation of their expression with E-cadherin expression: Hnf1b, Sim1, Tcfap2a, Emx2 and Grhl2 (Fig. 1A). We decided to focus our further characterization on Grhl2, because transcription factors of the grainyhead family had previously been implicated in the regulation of epithelial junctional components, which made Grhl2 an attractive candidate for a trans-activator of E-cadherin expression.

As predicted from our microarray screen, Grhl2 was highly expressed in the ureteric bud of the developing kidney (Fig. 1B; see Fig. S3A,B in the supplementary material). In addition, Grhl2 was expressed in the developing distal tubule, but not in glomerular or other proximal nephron epithelia. Grhl2 expression was maintained in the distal nephron in the adult kidney (see Fig. S3C-N in the supplementary material). A similar distal-to-proximal gradient of expression across the nephron is known for E-cadherin. Co-localization of Grhl2 and E-cadherin was illustrated by co-staining in the developing kidney where Grhl2-positive cells revealed marked E-cadherin positivity (Fig. 1B).

A screen of several cell lines for expression of Grhl2 revealed high expression levels (based on mRNA expression levels) in differentiated epithelial cell lines (e.g. MDCK, MCF-7 and mIMCD-3), but low expression levels in de-differentiated or non-epithelial cell lines (e.g. NIH-3T3) (see Fig. S4A in the

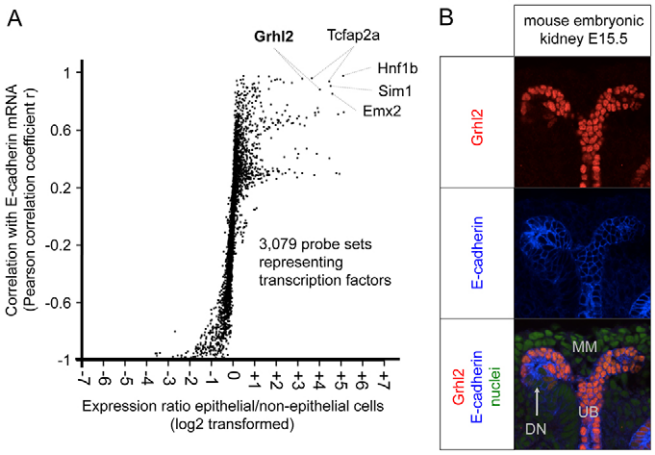

Fig. 1. Grhl2 is highly expressed in epithelial cells and co-regulated with E-cadherin. (**A**) Microarray-based screen for epithelial-specific transcription factors co-regulated with E-cadherin. All probe sets representing transcription factors were analyzed for differential expression in epithelial versus non-epithelial cells and Pearson correlation coefficient r was calculated between the probe set of each transcription factor and the probe set representing E-cadherin across all microarrays. The probe sets representing transcription factors that are highly overexpressed in epithelial cells and co-regulated with E-cadherin are labeled. (**B**) Grhl2 and E-cadherin are co-expressed in the developing kidney (E15.5) as detected by immunofluorescence staining. UB, ureteric bud; MM, metanephric mesenchyme; DN, distal nephron.

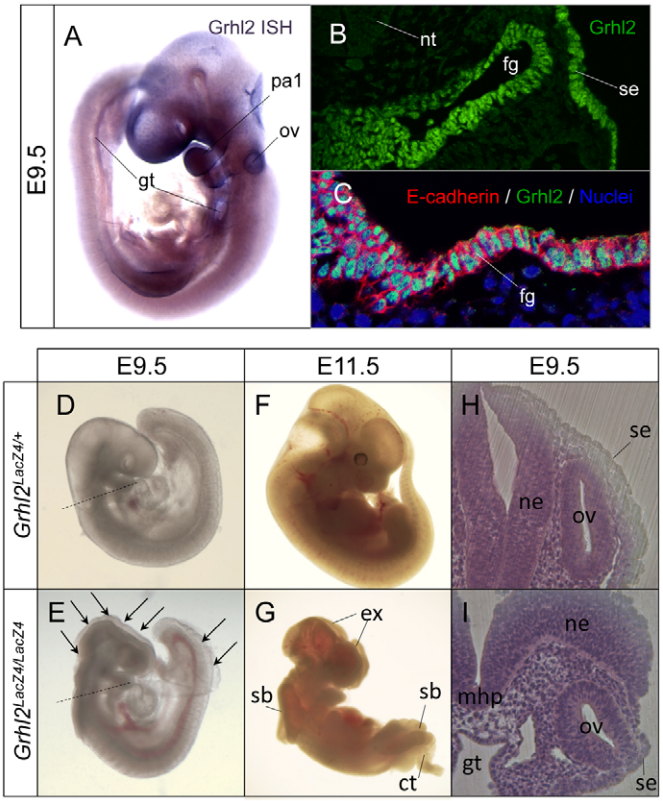

Fig. 2. *Grhl2* mutant mice display neural tube defects and exencephaly. (**A**) Whole-mount in situ hybridization revealing *Grhl2* expression in surface ectoderm, gut tube (gt) and otic vesicle (ov). (**B**) Immunofluorescence staining using a Grhl2 antibody revealing nuclear expression of Grhl2 in E9.5 foregut (fg) and surface ectoderm (se). The neural tube (nt) is Grhl2 negative. (**C**) Grhl2 colocalizes with E-cadherin as illustrated by immunofluorescence co-staining in the foregut (fg). (**D-I**) *Grhl2* mutant mice develop exencephaly and spina bifida. Although heterozygotes (*Grhl2*$^{LacZ4/+}$) develop normally (D,F), *Grhl2* homozygous mutants (*Grhl2*$^{LacZ4/LacZ4}$) display an open neural tube in the anterior and posterior region of the embryo at E9.5 (E, arrows) and develop manifest exencephaly (ex), anterior and posterior spina bifida (sb), and a curled tail (ct) at E11.5 (G). (H,I) Transverse sections at the level of the otic vesicle in E9.5 embryos (plane of sectioning indicated by broken lines in D and E) indicate that formation of the median hinge point (mhp) has occurred normally, but that neural fold elevation has failed in *Grhl2* mutants resulting in convexity of the neural folds. ne, neuroepithelium.

supplementary material). Similarly, Grhl2 expression in human tissue samples, including adult kidney, embryonic kidney, renal cell carcinomas and Wilms tumors was highly correlated with E-cadherin expression (see Fig. S4B in the supplementary material).

Grhl2 mutant mice exhibit defective epithelial differentiation and neural tube defects

To analyze the functional significance of Grhl2, we generated mice deficient for Grhl2. We obtained two independent embryonic stem (ES) cell lines with gene traps of the Grhl2 gene. In these cells, a splice acceptor followed by a β-galactosidase/neomycin resistance fusion gene (β-Geo) is inserted into intronic regions of the Grhl2 gene, which leads to aberrant splicing and premature termination of the Grhl2 transcript following exon 1 and 4, respectively. For simplicity, alleles were named Grhl2$^{LacZ1/+}$ (intron 1 trapped) and Grhl2$^{LacZ4/+}$ (intron 4 trapped) (see Fig. S1 in the supplementary material). Mouse mutants were generated from these ES cells.

Heterozygous Grhl2$^{LacZ1/+}$ and Grhl2$^{LacZ4/+}$ mice were viable and fertile. A detailed analysis of the Grhl2 expression pattern in vivo revealed overlapping expression domains for Grhl2 mRNA, Grhl2 protein and β-galactosidase expressed from the Grhl2 locus in Grhl2$^{LacZ1/+}$ mice (Fig. 2A-C; see Fig. S3 and Fig. S5A-C in the supplementary material). When Grhl2$^{LacZ4/+}$ were compared with Grhl2$^{LacZ1/+}$ mice, they exhibited lower β-galactosidase activity. At E8.5 to E9.5, Grhl2 was expressed in the surface ectoderm, the gut tube endoderm, the otic cup and nascent otic vesicle (Fig. 2A-C; see Fig. S5A-C in the supplementary material). These findings were consistent with previously published expression domains of Grhl2 (Auden et al., 2006).

Both Grhl2^{LacZ1} and Grhl2^{LacZ4} were null alleles. No residual Grhl2 mRNA could be detected using RT-PCR in embryo extracts from Grhl2$^{LacZ1/LacZ1}$ and Grhl2$^{LacZ4/LacZ4}$ mice (see Fig. S5D,E in the supplementary material). Although Grhl2 protein was present and displayed a nuclear localization in wild-type mice when analyzed by immunostaining with an antibody targeting the N-terminal region of Grhl2, no staining was observed in Grhl2$^{LacZ1/LacZ1}$ mice and staining was entirely cytoplasmic in Grhl2$^{LacZ4/LacZ4}$ mice (corresponding to the N terminus of Grhl2 encoded by exons 1-4 fused to β-Geo) (see Fig. S5F-I in the supplementary material).

Grhl2$^{LacZ1/LacZ1}$ and Grhl2$^{LacZ4/LacZ4}$ mice exhibited an identical and characteristic phenotype (Fig. 2D-I; see Fig. S5J-Q in the supplementary material): although embryo axial rotation was completed and neural tube closure initiated in mutant mice, cranial neural tube closure was not achieved, which resulted in anterior spina bifida, exencephaly and split face malformation (Fig. 2E,G). In addition, posterior neural tube closure failed, which resulted in lumbosacral spina bifida and an irregularly curled tail (a

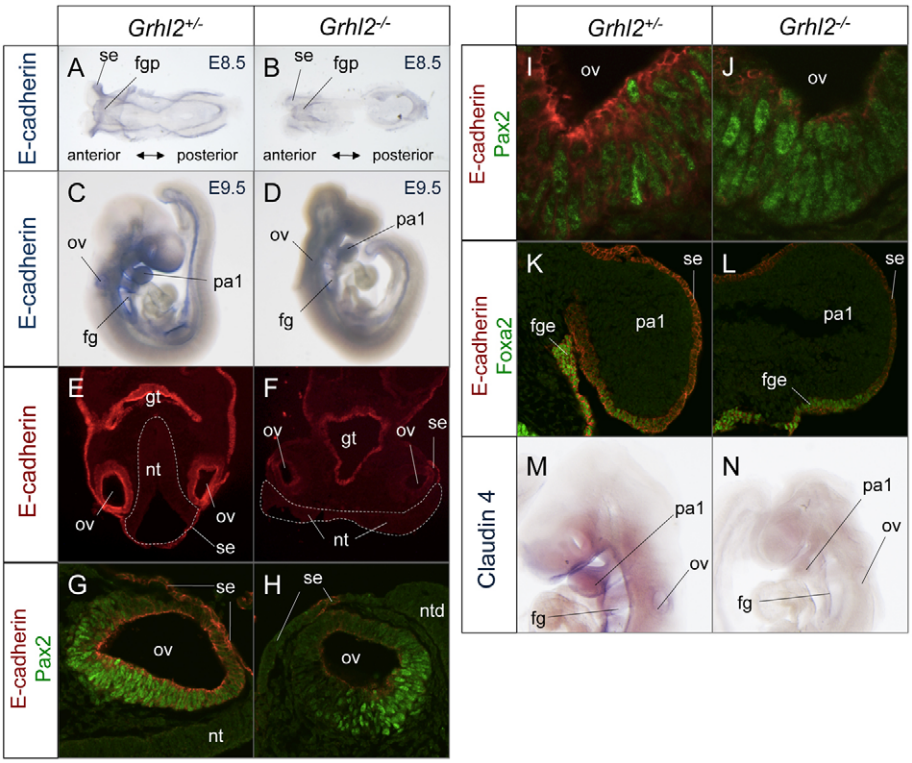

Fig. 3. Defective epithelial differentiation in *Grhl2* mouse mutants. (**A-D**) Whole-mount in situ hybridization for E-cadherin mRNA in E8.5 (A,B) and E9.5 (C,D) *Grhl2* mutant embryos (*Grhl2*$^{-/-}$) (B,D) and littermate controls (A,C). se, surface ectoderm; fgp, foregut pocket; ov, otic vesicle; fg, foregut; pa1, pharyngeal arch 1. (**E**,**F**) Transverse sections of E9.5 embryos at the level of the otic vesicle stained for E-cadherin protein revealing failure of neural tube (nt) closure and reduced E-cadherin levels in surface ectoderm (se), otic vesicle (ov) and gut tube (gt) in *Grhl2* mutants. (**G-J**) E-cadherin (red) and Pax2 (green) immunofluorescent co-staining in E9.5 otic vesicles in *Grhl2* mutants (H,J) and control littermates (G,I). (**K**,**L**) E-cadherin (red) and Foxa2 (green) immunofluorescent staining in E9.5 embryos indicates reduced expression of E-cadherin in *Grhl2* mutants in foregut endoderm (fge, Foxa2-positive) and surface ectoderm (se, Foxa2-negative) at the level of pharyngeal arch 1 (pa1). (**M**,**N**) Cldn4 expression is substantially reduced in foregut (fg), pharyngeal arch 1 (pa1) and otic vesicle (ov) in E9.5 *Grhl2* homozygous mutants as detected by whole-mount in situ hybridization.

characteristic hallmark of lumbosacral neural tube defects) by E11.5. Transverse sections of E9.5 embryos at the level of the anterior neural tube defect indicated that the neural plate had furrowed normally with formation of a median hinge point, but that neural fold elevation had not occurred (Fig. 2H,I). Consequently, the neuroepithelium remained convex (Fig. 2I).

Grhl2 mutants developed at a comparable pace with non-mutant littermates up to Theiler Stage 15 (~22 somites), when closure of the anterior neuropore was completed in non-mutant mice, indicating that the neural tube defects were not a result of developmental delay. Thereafter, we observed a progressive developmental retardation in Grhl2 mutants when compared with non-mutant littermates (Fig. 2D-G; see Fig. S5J-Q in the supplementary material). Embryo death occurred around day E11.5. No viable embryos were recovered at later stages.

The phenotype of Grhl2 mutant embryos and the co-expression of Grhl2 and E-cadherin were consistent with a role of Grhl2 in regulating epithelial differentiation and composition of epithelial junctions. Notably, Grhl2 is not expressed in the neural tube itself, but in adjacent surface ectoderm and in the gut tube. It has been reported that Grhl3 mutant mice display lumbosacral neural tube defects and a curled tail (Ting et al., 2003), similar to what we now report in Grhl2 mutants. Different mechanisms have been proposed for the neural tube defects in Grhl3 mutants, including epithelial defects in gut tube and surface ectoderm (Gustavsson et al., 2008; Hislop et al., 2008).

Drosophila Grainyhead and mouse Grhl1 and Grhl3 had been previously reported to regulate expression of epithelial junction components (Almeida and Bray, 2005; Narasimha et al., 2008; Wilanowski et al., 2008; Yu et al., 2006). Furthermore, E-cadherin expression has been previously linked with border cell migration and epithelial remodeling during morphogenesis (Geisbrecht and Montell, 2002; Gumbiner, 2005; Tinkle et al., 2004), functions that may be perturbed in Grhl2-deficient embryos based on the observed phenotype. Hence, we analyzed the molecular composition of the epithelial apical junctional complex in Grhl2 mutants. As previously reported (Stemmler et al., 2005), E-cadherin was expressed in surface ectoderm and gut endoderm at E8.5 in wild-type or heterozygous mice (Fig. 3A) and became concentrated in the ectoderm of the head region at E9.5 with particularly high levels in surface ectoderm, foregut endoderm and otic cup/otic vesicle epithelium (Fig. 3C,E). This expression pattern was virtually identical with the expression pattern we had observed for Grhl2. By contrast, E-cadherin expression in Grhl2 mutants was substantially reduced in several types of epithelia (Fig. 3A-L). In E8.5 Grhl2 mutants, the E-cadherin expression domain in the surface ectoderm of the presumptive head region was substantially contracted and those regions that maintained E-cadherin expression did so at a lower level when compared with non-mutant littermates (Fig. 3A,B). At E9.5, the expression domain of E-cadherin in the cranial surface ectoderm was markedly reduced (Fig. 3C,D). Otic vesicles formed in Grhl2 mutants, but E-cadherin expression was substantially reduced in the otic epithelium (Fig. 3C-J). The foregut endoderm and the surface ectoderm also displayed reduced E-cadherin expression (Fig. 3K,L).

Claudin 4 (Cldn4) is another marker of epithelial differentiation that is known to be expressed in otic and foregut epithelia and part of the surface ectoderm with an expression domain very similar to that of Grhl2 (Burtscher and Lickert, 2009). Hence, we analyzed Cldn4 expression by in situ hybridization and found that it was markedly reduced across all epithelia in Grhl2 mutants (Fig. 3M,N). Conversely, analysis of markers of foregut (Foxa2) and otic (Pax2) epithelia in Grhl2 mutants indicated that the initial patterning and specification of these epithelia was intact (Fig. 3G-L).

The epithelial morphology and membrane localization of residual E-cadherin in Grhl2-deficient epithelia suggested that an apical junctional complex was formed, but exhibited defective molecular composition. We analyzed key components of the apical

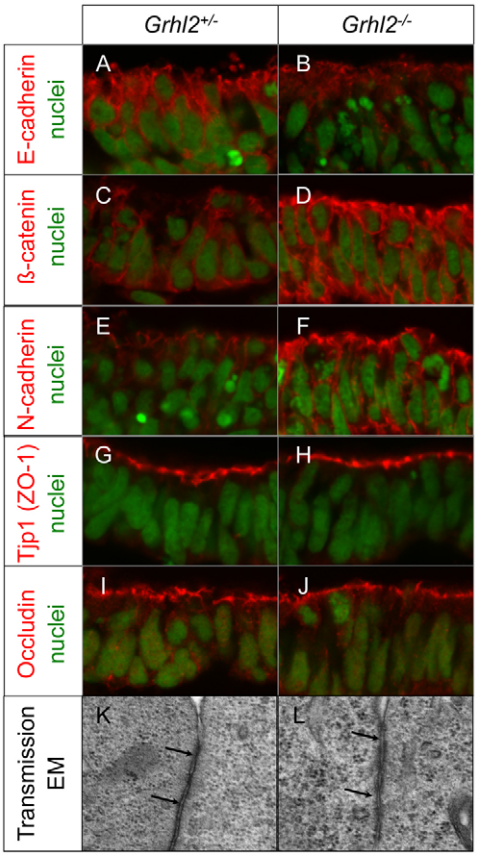

Fig. 4. Defective molecular composition of the apical junctional complex in *Grhl2* mutant mice. High power visualization of immunofluorescence staining for E-cadherin (**A**,**B**), β-catenin (**C**,**D**), N-cadherin (**E**,**F**), Tjp1 (**G**,**H**) and occludin (**I**,**J**) in otic vesicle epithelia at E9.5. (**K**,**L**) Transmission electron microscopy (12,500×) of otic vesicle epithelia (luminal side on top) reveals no overt structural abnormalities of the apical junctional complex (arrows) at this stage.

junctional complex in Grhl2-deficient otic vesicle epithelia in E9.5 embryos. Although E-cadherin was reduced in Grhl2 mutants (Fig. 4A,B), β-catenin was appropriately localized to the cell membrane (Fig. 4C,D), suggesting that another classical cadherin was present to recruit β-catenin to the lateral membrane. Indeed, we found upregulation of N-cadherin in Grhl2-deficient epithelia (Fig. 4E,F), suggesting that N-cadherin (and possibly also other classical cadherins) participates in the maintenance of adherens junctions in Grhl2-deficient epithelia. Tight junctions markers displayed an intact apical localization, as determined by occludin and tight junction protein 1 (Tjp1, also known as ZO-1) staining (Fig. 4G-J). In addition, transmission electron microscopy of these epithelia indicated that the apical junctional complex was structurally intact at this stage (Fig. 4K,L). Together, these observations indicate that Grhl2 mutant mice have a specific defect of epithelial differentiation and, despite apparent structural integrity, display defective molecular composition of the apical junctional complex.

Mechanistic insights into target gene regulation by Grhl2

To analyze the molecular basis of the epithelial differentiation defect as a result of Grhl2 deficiency, we used mIMCD-3 cells, which display robust Grhl2 expression and express comparatively low levels of the other Grhl isoforms Grhl1 and Grhl3 (see Fig. S6 in the supplementary material). We generated mIMCD-3 cells with a knockdown of Grhl2 by stably introducing plasmids overexpressing shRNAs that target Grhl2 (Fig. 5). These Grhl2 knockdown (Grhl2-kd) cells phenocopied the epithelial defects observed in vivo. Compared with control mIMCD-3 cells, Grhl2-kd cells displayed reduced expression of E-cadherin mRNA and protein (Fig. 5A-C), but exhibited normal membrane localization of β-catenin and increased levels of N-cadherin (Fig. 5B). Similar to Grhl2-deficient cells in vivo, Cldn4 expression was substantially reduced in Grhl2-kd cells (Fig. 5A,B). E-cadherin expression was rescued in Grhl2 knockdown cells after transient transfection of an shRNA-resistant full-length Grhl2, indicating specificity of the effect (Fig. 5D).

We hypothesized that Grhl2 regulates E-cadherin and Cldn4 expression via direct interaction with these genes. As the Grhl2 homologs Grhl1 and Grhl3, as well as *Drosophila* Grainyhead, all share a similar DNA-binding consensus sequence (Ting et al., 2005; Venkatesan et al., 2003; Wilanowski et al., 2008), we mapped the cis-regulatory sequences sufficient to drive E-cadherin-specific expression in endodermal and ectodermal epithelia (–1.5 kb to +11 kb) (Stemmler et al., 2003) for occurrences of the published Grainyhead consensus motif that were conserved in mice, humans and dogs by mapping of multiple-sequence alignments between the three species (Ovcharenko et al., 2005). We found a single Grainyhead consensus site located in intron 2 of the E-cadherin gene 7768 bp downstream from the TSS (see Fig. S7 in the supplementary material). The site displayed two adjacent Grainyhead consensus sequences positioned in a tandem formation and was conserved in mammals. No additional conserved Grainyhead sites were found within the E-cadherin gene and between E-cadherin and its neighboring genes. A similarly structured and conserved putative Grainyhead-binding site was identified at the Cldn4 core promoter (Fig. 6). To detect Grhl2-DNA association at these putative binding sites, we used chromatin immunoprecipitation (ChIP) on mIMCD-3 cells and on mouse kidney extracts (Fig. 6A, Fig. 7A; see Fig. S8 in the supplementary material). The results revealed specific enrichment of Grhl2-DNA binding at the predicted binding sites at the Cldn4 promoter and in intron 2 of the E-cadherin gene, while background levels of Grhl2-DNA association were detected at the E-cadherin promoter and at additional control sites. Hence, we conclude that Grhl2 specifically associates with DNA motifs localized at the Cldn4 promoter and in intron 2 of the E-cadherin gene.

The N-terminal domains of Grainyhead-related proteins have previously been implicated in transcriptional activation, while the C-terminal regions harbor DNA binding and dimerization domains (Attardi et al., 1993; Uv et al., 1994; Wilanowski et al., 2002). Deletion of the N-terminal domains of *Drosophila* Grainyhead or of *Xenopus* Grhl1 produces dominant-negative mutant proteins that compete with endogenous proteins for DNA interaction and inhibit the transcriptional activation of target genes (Attardi et al., 1993; Tao et al., 2005). To test whether mouse Grhl2 functions analogously, we deleted the N-terminal domain and replaced it with GFP, hypothesizing that this would result in a dominant-negative DNA-binding protein (Dn-Grhl2) (see Fig. S9A in the supplementary material). Overexpression of Dn-Grhl2 in mIMCD-3 cells resulted in downregulation of E-cadherin and Cldn4 expression (see Fig. S9B,C in the supplementary material). Using ChIP, we found that endogenous Grhl2 was displaced from intron 2 of the E-cadherin gene following overexpression of Dn-Grhl2 (see Fig. S9D in the supplementary material). Instead, Dn-Grhl2 associated with this site, as demonstrated by ChIP using a GFP antibody that recognizes the N terminus of the Dn-Grhl2 protein

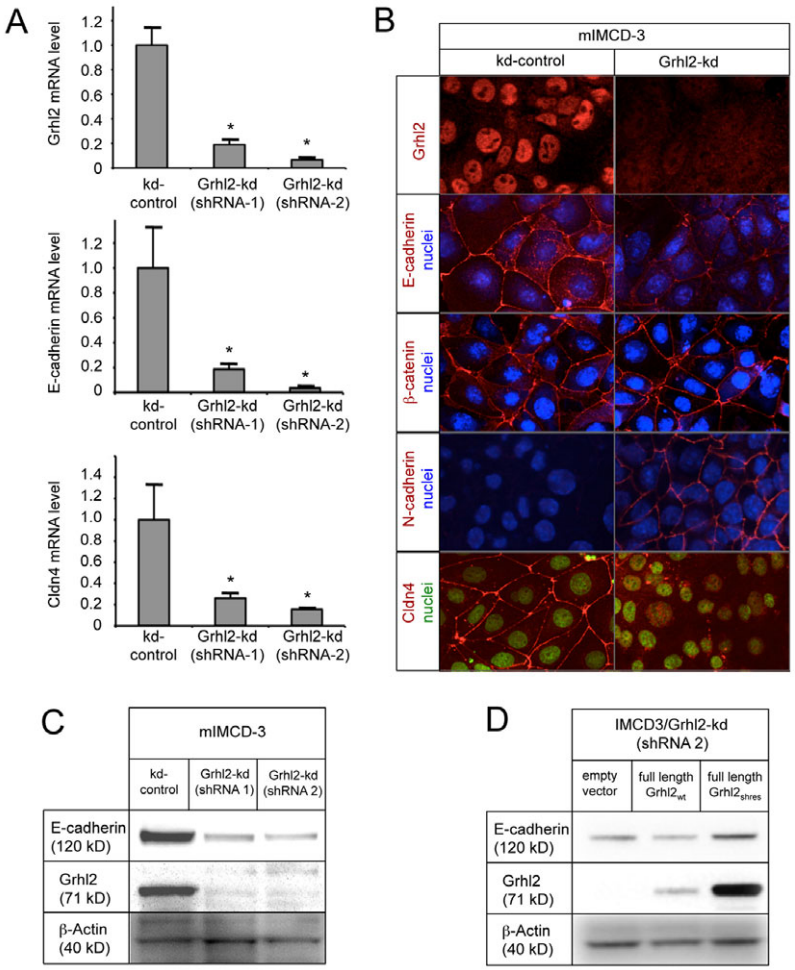

Fig. 5. *Grhl2* knockdown in mIMCD-3 cells alters apical junctional complex composition. (**A**) Real-time RT-PCR for *Grhl2* mRNA, E-cadherin mRNA and Cldn4 mRNA in mIMCD-3 cells transfected with control shRNA (kd-control) or with different shRNAs targeting Grhl2 (Grhl2-kd; shRNA-1 and shRNA-2). Each bar represents at least four different biological replicates. **P*<0.05 versus kd-control. (**B**) Immunofluorescent staining reveals decreased levels of Grhl2, E-cadherin and Cldn4, but normal levels of β-catenin and increased levels of N-cadherin in Grhl2-kd cells when compared with kd-control cells. (**C**) Western blot analysis of Grhl2 and E-cadherin protein expression in Grhl2-kd and kd-control cells reveals knockdown of Grhl2 and reduction of E-cadherin protein in Grhl2-kd cells. **P*<0.05 versus kd-control, *n*=3. (**D**) Transient transfection of a full-length shRNA-resistant Grhl2 ($Grhl2_{shres}$) into Grhl2-kd cells reinduces E-cadherin expression after 3 days of culture, whereas a full-length wild-type Grhl2 ($Grhl2_{wt}$) is efficiently degraded by the shRNA and fails to reinduce E-cadherin expression. **P*<0.05 versus empty vector, *n*=3.

(see Fig. S9D in the supplementary material). Hence, as previously suggested (Wilanowski et al., 2002), Grhl2 appears to function similar to its homolog Grhl1 in inducing target gene expression via an N-terminal transcriptional activation domain.

We hypothesized that Grhl2 binding to the E-cadherin and Cldn4 genes would directly affect transcriptional activity at the respective loci. To test the functional relevance of Grhl2 binding to the Cldn4 promoter, we constructed a reporter plasmid containing Cldn4 regulatory regions from –611 bp to +174 bp relative to the TSS. We found strongly enhanced reporter activity in mIMCD-3 control cells transfected with this plasmid when compared with an empty reporter vector (Fig. 6B). Reporter activity was substantially reduced in Grhl2-kd cells, indicating that Cldn4 promoter activity is strongly Grhl2 dependent (Fig. 6B). In addition, deletion or mutagenesis of the Grhl2-binding site resulted in substantially decreased promoter activity in mIMCD-3 cells (Fig. 6C). Together, these data indicate that Grhl2 is a required component of the transcriptional machinery that transactivates the Cldn4 promoter.

In the case of E-cadherin, we observed intronic association of Grhl2. Notably, the E-cadherin intronic region associated with Grhl2 had previously been shown to be required and sufficient for tissue-specific E-cadherin transcription in vivo (Stemmler et al., 2005; Stemmler et al., 2003). We hypothesized that the Grhl2-binding region in intron 2 of the E-cadherin gene would interact with the promoter to locally regulate promoter activity. To assay for chromatin looping between the Grhl2-associated enhancer in intron 2 and the promoter, we applied chromatin conformation capture (3C), which allows detection of physical interaction between distant chromosomal elements in vivo (Dekker et al., 2002). We applied a semi-quantitative 3C protocol to mIMCD-3 cells (Fig. 7B). The method is based on crosslinking of cell extracts followed by complete restriction digestion with *Bgl*II and religation using T4 ligase. DNA fragments in physical proximity are more likely to religate than distant fragments. Religation of *Bgl*II fragments corresponding to given genomic sites is detected by PCR using primer pairs spanning the *Bgl*II restriction site. We detected religation between the *Bgl*II fragment encompassing the Grhl2-bound site in intron 2 and the *Bgl*II fragment encompassing the E-cadherin promoter. To assay for specificity of this interaction, we analyzed religation between the E-cadherin promoter and a negative control locus at a similar distance upstream from the E-cadherin gene. To avoid differences in the primer binding efficiencies and non-linearity of the PCR reaction, we analyzed amplification efficiency for each primer set using digested and religated BAC DNA containing mouse E-cadherin genomic sequences. As a positive control, we assayed established interacting chromatin regions at the GAPDH locus. The experiments demonstrated a physical interaction between the E-cadherin promoter and the fragment of intron 2 containing the Grhl2 binding site (Fig. 7B).

We hypothesized that Grhl2, through direct association with intron 2 of the E-cadherin gene and loop-mediated contact with the E-cadherin promoter, participates in remodeling of the E-cadherin promoter. To test this hypothesis, we analyzed histone H3-K4 tri-methylation (H3-K4-Me3) and histone H3-K9/14 acetylation (H3-

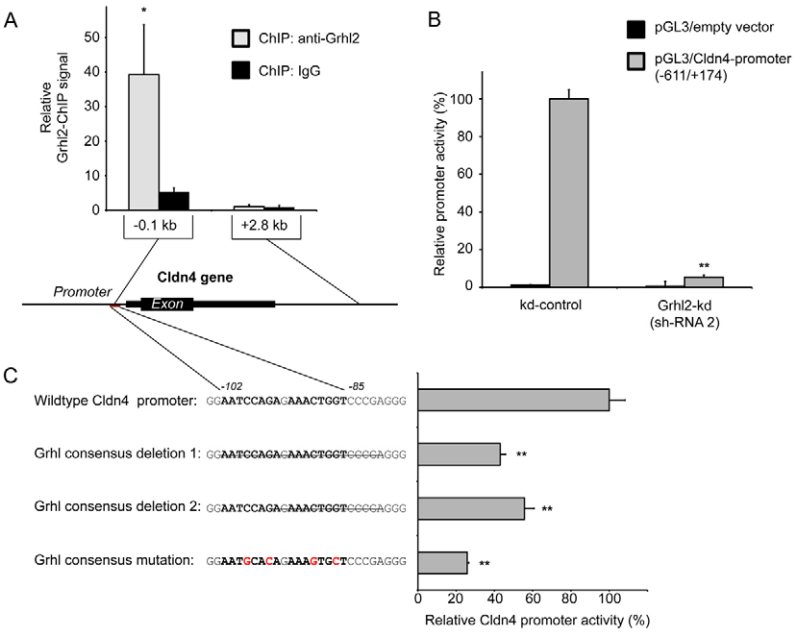

Fig. 6. Grhl2 transactivates Cldn4 expression via association with the core promoter. (**A**) ChIP-PCR assay in mIMCD-3 cells to detect binding of Grhl2 within the Cldn4 promoter region (–0.1 kb). Relative binding is compared with a negative control locus (+2.8 kb) and normalized to input. **P*<0.05 versus control locus. (**B**) Luciferase assays were carried out to assay activity of a promoter construct encompassing bases –611 to +174 relative to the Cldn4 TSS. This was compared with an empty reporter vector (pGL3-empty) in kd-control cells and Grhl2-kd cells. ***P*<0.01 versus kd-control. (**C**) The Grhl consensus sequence was deleted or mutagenized as indicated. Promoter activity in mIMCD-3 cells was compared with the wild-type Cldn4 promoter construct. ***P*<0.01 versus wild-type Cldn4 promoter (ANOVA with post-hoc Dunnett's test).

K9/14-Ac), two characteristic marks of active chromatin (Liang et al., 2004) in control cells and Grhl2-kd cells. Control cells displayed high levels of these histone modifications at the E-cadherin promoter, but not at other sites across the gene, including the Grhl2 binding site (Fig. 7A). Following knockdown of Grhl2, H3-K4-Me3 and H3-K9/14-Ac were significantly reduced at the E-cadherin promoter, indicating that Grhl2 was required in these cells to maintain activating histone marks at the promoter (Fig. 7A).

DISCUSSION

Our study provides several novel findings: we identified Grhl2 in a genome-wide screen as one of very few transcription factors tightly co-regulated with E-cadherin across different cell types and tissues. We showed that Grhl2 functions to regulate epithelial differentiation in different types of epithelia both in vivo and in vitro and found that Grhl2 deficiency in mice results in defective neural tube closure and in embryonic lethality by E11.5. Finally, we provided molecular evidence that Grhl2 acts as a transcription factor that specifically associates with DNA motifs in the promoter of Cldn4 and in the second intron of the E-cadherin gene to regulate expression levels of these genes.

Grhl2 functions in vivo to regulate epithelial differentiation in the otic vesicle, the gut endoderm and surface ectoderm. Molecularly, Grhl2-deficient epithelia display decreased expression of E-cadherin and Cldn4. Both proteins are known to serve as surrogate markers of epithelial differentiation (Burtscher and Lickert, 2009; Gumbiner, 2005). Functionally, Grhl2 deficiency results in defective neural tube closure in the entire anterior part of the embryo and in the lumbosacral region. Notably, Grhl2 is not expressed in the neural tube itself, but in adjacent surface ectoderm and in the gut tube. In this regard, Grhl2 shows an obvious similarity to its mammalian homolog Grhl3 (Get1), a gene known to be important for neural tube closure, epidermal integrity, wound healing and eye lid closure (Harris, 2009; Hislop et al., 2008; Ting et al., 2005; Ting et al., 2003; Yu et al., 2008; Yu et al., 2006). Given the similar, partially overlapping expression domains of Grhl2 and Grhl3, similar mechanisms are likely to account for the neural tube defects in Grhl2 and Grhl3 mutants. Although Grhl3 mutants usually display neural tube defects in the lumbosacral region only, anterior neural tube defects and exencephaly are rare events in Grhl3 mutants (Ting et al., 2003). By contrast, we observed anterior and posterior neural tube defects, including exencephaly, in all Grhl2 homozygous mutant embryos analyzed (n>30), which indicates a more severe and highly penetrant phenotype. Unlike Grhl3 mutants, Grhl2 mutants do not live to birth, because they display progressive developmental retardation after E9.5, resulting in embryonic lethality around E11.5. Our data (K.W. and K.M.S.O., unpublished) indicate that this phenotype is related to a placental defect.

Our data provide evidence that Grhl2 directly participates in the regulation of Cldn4 and E-cadherin expression. We found that Grhl2 transactivates Cldn4 via direct association with a DNA consensus motif within the Cldn4 core promoter, as demonstrated by ChIP. Knockdown of Grhl2 or mutagenesis of the corresponding cis-regulatory element led to a strong reduction of Cldn4 promoter activity, indicating that Grhl2 acts as a direct transcriptional activator of Cldn4.

Our data also show that Grhl2 binds to a previously characterized cis-regulatory region localized in intron 2 of the E-cadherin gene. Previous functional analyses of E-cadherin transcriptional regulation revealed that a deletion of the entire intron 2 (spanning 45 kb of genomic sequences) resulted in an absence of E-cadherin-specific reporter expression during early mouse embryogenesis (Stemmler et al., 2005). In addition, when sequences from +0.1 to +11 kb from the TSS of the E-cadherin gene (including the first 10 kb of intron 2) were combined with the core promoter in transgenic reporter assays, epithelial-specific enhancer activity was observed in endodermal and ectodermal epithelia (Stemmler et al., 2003). Together, these studies indicate that the first 10 kb of intron 2 contain crucial elements for E-cadherin regulation. The Grhl2-binding site we identified is localized within this region, 6.7 kb downstream from the start of intron 2. Our chromatin conformation capture data indicate that this Grhl2-associated cis-regulatory element localizes in physical proximity to the E-cadherin promoter as a result of chromatin looping. Furthermore, our ChIP data indicate that activating histone modifications at the E-cadherin promoter are specifically reduced

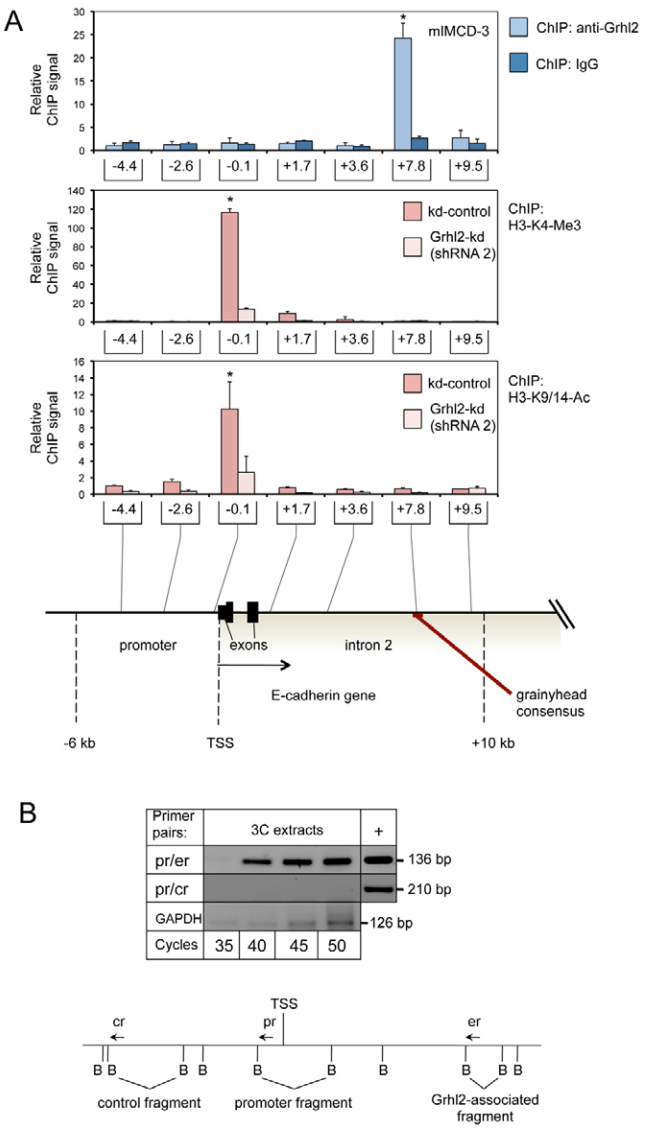

Fig. 7. Grhl2 binds to an intronic enhancer of the E-cadherin gene. (**A**) Mapping of the E-cadherin locus by ChIP-PCR. ChIP using Grhl2 antibody or immunoglobulin G (IgG; negative control) on mIMCD-3 cells reveals enrichment of DNA sequences at the grainyhead consensus site in intron 2 when compared with other regions of the E-cadherin gene, including the promoter. Levels of histone H3-K4 trimethylation (H3-K4-Me3) and H3-K9/14 acetylation (H3-K9/14-Ac) at the E-cadherin promoter (–0.1 kb) are reduced in Grhl2-kd cells. **P*<0.01 versus IgG or Grhl2-kd. (**B**) Chromatin conformation capture following digestion of formalin-crosslinked mIMCD-3 cell extracts with *Bgl*II and religation using T4 ligase. Scheme indicates *Bgl*II sites (B) at the E-cadherin locus in relation to the TSS. Arrows indicate the locations of the 3C primers. The 136 bp PCR product reflects religation between the *Bgl*II fragment encompassing the E-cadherin promoter and the *Bgl*II fragment encompassing the Grhl2-binding site (genomic distance between religated ends is 8,392 bp), indicating that these fragments reside in physical proximity. This is compared with a 210 bp PCR fragment detecting religation between the *Bgl*II fragment encompassing the E-cadherin promoter and a *Bgl*II fragment upstream from the TSS (genomic distance between religated ends is 6,230 bp), which serves as a negative control. Two fragments 559 bp apart at the GAPDH locus serve as a ligation control (Spilianakis and Flavell, 2004). A BAC clone containing the mouse E-cadherin locus digested with *Bgl*II and religated with T4 ligase serves as a positive control template for each PCR reaction (+).

in Grhl2-deficient cells. Together, these observations are consistent with a model where Grhl2 binds to intron 2 of the E-cadherin gene and, via chromatin looping, contacts and remodels the E-cadherin promoter (see Fig. S10 in the supplementary material). However, we acknowledge that functional proof of the necessity of the Grhl2-associated cis-regulatory element in intron 2 for E-cadherin expression in vivo (by mutagenesis) is still lacking.

Interestingly, we found that Grhl2-deficient epithelia displayed markedly upregulated N-cadherin expression, which may explain the apparent structural integrity of the adherens junction in these cells. Multiple mechanisms could account for this N-cadherin upregulation upon loss of Grhl2 function. Grhl2 may directly repress N-cadherin or positively regulate an N-cadherin repressor. Alternatively, upregulation of N-cadherin may be the result of a reduced E-cadherin expression. In this context, it is interesting to note that a knockdown of E-cadherin in cultured epithelial cells results in a marked upregulation of N-cadherin (Onder et al., 2008).

Grainyhead-related factors have previously been implicated in the regulation of epithelial junctional genes. *Drosophila* Grainyhead has been implicated in the regulation and of septate junction components (Narasimha et al., 2008). Notably, *Drosophila* Shotgun, which is widely considered to be a homolog of E-cadherin (Tepass et al., 1996), has been reported to be downregulated in postembryonic neuroblasts in grainyhead mutant flies (Almeida and Bray, 2005). However, the cis-regulatory region in intron 2 of the E-cadherin gene is not conserved beyond placental mammals; hence, E-cadherin regulation by Grhl2 must be mammalian specific. Grhl3 is involved in terminal differentiation of epidermal and urothelial epithelia and does so by activating terminal differentiation-associated genes via direct promoter binding (Yu et al., 2006; Yu et al., 2009). Similarly, Grhl1 regulates desmoglein 1, a desmosomal cadherin, and is central for structural integrity of the epidermis (Wilanowski et al., 2008). In a recent report by Yu et al., E-cadherin mRNA was 1.3-fold downregulated in the epidermis in E18.5 Grhl3 mutant mice compared with non-mutant littermates according to microarray analysis (Yu et al., 2009). Although the result did not reach statistical significance (P=0.09), it suggests that Grhl3 may also participate in E-cadherin regulation. Conversely, no significant changes in E-cadherin expression were observed in the epidermis of Grhl1 mutant mice (Wilanowski et al., 2008). These data suggest that Grhl2 and Grhl3 may perform redundant functions in the regulation of E-cadherin, which is consistent with the observation that Grhl2 and Grhl3 mutant mice exhibit similar phenotypes.

Although we first identified Grhl2 in epithelia of the developing kidney and in mIMCD-3 cells derived from the renal collecting duct, the embryonic lethality of the Grhl2 mutant mice has thus far precluded a meaningful analysis of kidney development, which is initiated at E10.5, when we already observe a substantial developmental delay in Grhl2 mutants. To circumvent the embryonic lethality and specifically analyze the role of Grhl2 in kidney epithelia, we are currently in the process of generating a conditional Grhl2 allele in mice.

Taken together, our data support the notion that Grhl2 is a direct transactivator of apical junctional complex components. In this regard, Grhl2 resembles hepatocyte nuclear factor 4α (Hnf4a), a transcription factor that regulates epithelial differentiation and orchestrates expression of several cell adhesion molecules, including E-cadherin and various claudins (Battle et al., 2006; Parviz et al., 2003). Interestingly, a recent genome-wide survey of Hnf4a binding sites in liver indicated the presence of several binding peaks in intron 2 of the E-cadherin gene, one of them at a distance of less than 500

bp from the Grhl2 binding site we detected (Schmidt et al., 2010). Our future studies will further explore the relation of Grhl2 to other regulators of epithelial differentiation and the genome-wide target gene program regulated by Grhl2.

Acknowledgements
This work was supported by DFG grants Schm1730/2-1 and Schm1730/3-1 to K.M.S.O. We thank Francesca Spagnoli, Thomas Willnow, Annette Hammes and Annabel Christ (all from MDC Berlin) for their help during the course of this study and for comments concerning the manuscript. We thank Anje Sporbert (MDC Berlin) for providing expertise in confocal microscopy imaging. We thank Antje Sommer and Tatjana Luganskaja for their excellent technical support.

Competing interests statement
The authors declare no competing financial interests.

Supplementary material
Supplementary material for this article is available at
http://dev.biologists.org/lookup/suppl/doi:10.1242/dev.055483/-/DC1

References
Almeida, M. S. and Bray, S. J. (2005). Regulation of post-embryonic neuroblasts by Drosophila Grainyhead. *Mech. Dev.* **122**, 1282-1293.
Attardi, L. D., Von Seggern, D. and Tjian, R. (1993). Ectopic expression of wild-type or a dominant-negative mutant of transcription factor NTF-1 disrupts normal Drosophila development. *Proc. Natl. Acad. Sci. USA* **90**, 10563-10567.
Auden, A., Caddy, J., Wilanowski, T., Ting, S. B., Cunningham, J. M. and Jane, S. M. (2006). Spatial and temporal expression of the Grainyhead-like transcription factor family during murine development. *Gene Expr. Patterns* **6**, 964-970.
Batlle, E., Sancho, E., Franci, C., Dominguez, D., Monfar, M., Baulida, J. and Garcia De Herreros, A. (2000). The transcription factor snail is a repressor of E-cadherin gene expression in epithelial tumour cells. *Nat. Cell Biol.* **2**, 84-89.
Battle, M. A., Konopka, G., Parviz, F., Gaggl, A. L., Yang, C., Sladek, F. M. and Duncan, S. A. (2006). Hepatocyte nuclear factor 4alpha orchestrates expression of cell adhesion proteins during the epithelial transformation of the developing liver. *Proc. Natl. Acad. Sci. USA* **103**, 8419-8424.
Behrens, J., Mareel, M. M., Van Roy, F. M. and Birchmeier, W. (1989). Dissecting tumor cell invasion: epithelial cells acquire invasive properties after the loss of uvomorulin-mediated cell-cell adhesion. *J. Cell Biol.* **108**, 2435-2447.
Burtscher, I. and Lickert, H. (2009). Foxa2 regulates polarity and epithelialization in the endoderm germ layer of the mouse embryo. *Development* **136**, 1029-1038.
Cano, A., Perez-Moreno, M. A., Rodrigo, I., Locascio, A., Blanco, M. J., del Barrio, M. G., Portillo, F. and Nieto, M. A. (2000). The transcription factor snail controls epithelial-mesenchymal transitions by repressing E-cadherin expression. *Nat. Cell Biol.* **2**, 76-83.
Carver, E. A., Jiang, R., Lan, Y., Oram, K. F. and Gridley, T. (2001). The mouse snail gene encodes a key regulator of the epithelial-mesenchymal transition. *Mol. Cell. Biol.* **21**, 8184-8188.
Comijn, J., Berx, G., Vermassen, P., Verschueren, K., van Grunsven, L., Bruyneel, E., Mareel, M., Huylebroeck, D. and van Roy, F. (2001). The two-handed E box binding zinc finger protein SIP1 downregulates E-cadherin and induces invasion. *Mol. Cell* **7**, 1267-1278.
Conacci-Sorrell, M., Simcha, I., Ben-Yedidia, T., Blechman, J., Savagner, P. and Ben-Ze'ev, A. (2003). Autoregulation of E-cadherin expression by cadherin-cadherin interactions: the roles of beta-catenin signaling, Slug, and MAPK. *J. Cell Biol.* **163**, 847-857.
Dekker, J., Rippe, K., Dekker, M. and Kleckner, N. (2002). Capturing chromosome conformation. *Science* **295**, 1306-1311.
Geisbrecht, E. R. and Montell, D. J. (2002). Myosin VI is required for E-cadherin-mediated border cell migration. *Nat. Cell Biol.* **4**, 616-620.
Grooteclaes, M. L. and Frisch, S. M. (2000). Evidence for a function of CtBP in epithelial gene regulation and anoikis. *Oncogene* **19**, 3823-3828.
Gumbiner, B. M. (2005). Regulation of cadherin-mediated adhesion in morphogenesis. *Nat. Rev. Mol. Cell Biol.* **6**, 622-634.
Gustavsson, P., Copp, A. J. and Greene, N. D. (2008). Grainyhead genes and mammalian neural tube closure. *Birth Defects Res. A Clin. Mol. Teratol.* **82**, 728-735.
Halbleib, J. M. and Nelson, W. J. (2006). Cadherins in development: cell adhesion, sorting, and tissue morphogenesis. *Genes Dev.* **20**, 3199-3214.
Hammes, A., Guo, J. K., Lutsch, G., Leheste, J. R., Landrock, D., Ziegler, U., Gubler, M. C. and Schedl, A. (2001). Two splice variants of the Wilms' tumor 1 gene have distinct functions during sex determination and nephron formation. *Cell* **106**, 319-329.
Harris, M. J. (2009). Insights into prevention of human neural tube defects by folic acid arising from consideration of mouse mutants. *Birth Defects Res. A Clin. Mol. Teratol.* **85**, 331-339.
Herrero, J., Al-Shahrour, F., Diaz-Uriarte, R., Mateos, A., Vaquerizas, J. M., Santoyo, J. and Dopazo, J. (2003). GEPAS: A web-based resource for microarray gene expression data analysis. *Nucleic Acids Res.* **31**, 3461-3467.
Hislop, N. R., Caddy, J., Ting, S. B., Auden, A., Vasudevan, S., King, S. L., Lindeman, G. J., Visvader, J. E., Cunningham, J. M. and Jane, S. M. (2008). Grhl3 and Lmo4 play coordinate roles in epidermal migration. *Dev. Biol.* **321**, 263-272.
Horn, C., Hansen, J., Schnutgen, F., Seisenberger, C., Floss, T., Irgang, M., De-Zolt, S., Wurst, W., von Melchner, H. and Noppinger, P. R. (2007). Splinkerette PCR for more efficient characterization of gene trap events. *Nat. Genet.* **39**, 933-934.
Larue, L., Antos, C., Butz, S., Huber, O., Delmas, V., Dominis, M. and Kemler, R. (1996). A role for cadherins in tissue formation. *Development* **122**, 3185-3194.
Liang, G., Lin, J. C., Wei, V., Yoo, C., Cheng, J. C., Nguyen, C. T., Weisenberger, D. J., Egger, G., Takai, D., Gonzales, F. A. et al. (2004). Distinct localization of histone H3 acetylation and H3-K4 methylation to the transcription start sites in the human genome. *Proc. Natl. Acad. Sci. USA* **101**, 7357-7362.
Meng, W. and Takeichi, M. (2009). Adherens junction: molecular architecture and regulation. *Cold Spring Harbor Perspect. Biol.* **1**, a002899.
Narasimha, M., Uv, A., Krejci, A., Brown, N. H. and Bray, S. J. (2008). Grainy head promotes expression of septate junction proteins and influences epithelial morphogenesis. *J. Cell Sci.* **121**, 747-752.
Onder, T. T., Gupta, P. B., Mani, S. A., Yang, J., Lander, E. S. and Weinberg, R. A. (2008). Loss of E-cadherin promotes metastasis via multiple downstream transcriptional pathways. *Cancer Res.* **68**, 3645-3654.
Ovcharenko, I., Loots, G. G., Giardine, B. M., Hou, M., Ma, J., Hardison, R. C., Stubbs, L. and Miller, W. (2005). Mulan: multiple-sequence local alignment and visualization for studying function and evolution. *Genome Res.* **15**, 184-194.
Parviz, F., Matullo, C., Garrison, W. D., Savatski, L., Adamson, J. W., Ning, G., Kaestner, K. H., Rossi, J. M., Zaret, K. S. and Duncan, S. A. (2003). Hepatocyte nuclear factor 4alpha controls the development of a hepatic epithelium and liver morphogenesis. *Nat. Genet.* **34**, 292-296.
Peinado, H., Marin, F., Cubillo, E., Stark, H. J., Fusenig, N., Nieto, M. A. and Cano, A. (2004). Snail and E47 repressors of E-cadherin induce distinct invasive and angiogenic properties in vivo. *J. Cell Sci.* **117**, 2827-2839.
Perez-Moreno, M. A., Locascio, A., Rodrigo, I., Dhondt, G., Portillo, F., Nieto, M. A. and Cano, A. (2001). A new role for E12/E47 in the repression of E-cadherin expression and epithelial-mesenchymal transitions. *J. Biol. Chem.* **276**, 27424-27431.
Schedl, A. (2007). Renal abnormalities and their developmental origin. *Nat. Rev. Genet.* **8**, 791-802.
Schmidt, D., Wilson, M. D., Ballester, B., Schwalie, P. C., Brown, G. D., Marshall, A., Kutter, C., Watt, S., Martinez-Jimenez, C. P., Mackay, S. et al. (2010). Five-vertebrate ChIP-seq reveals the evolutionary dynamics of transcription factor binding. *Science* **328**, 1036-1040.
Schmidt-Ott, K. M., Yang, J., Chen, X., Wang, H., Paragas, N., Mori, K., Li, J. Y., Lu, B., Costantini, F., Schiffer, M. et al. (2005). Novel regulators of kidney development from the tips of the ureteric bud. *J. Am. Soc. Nephrol.* **16**, 1993-2002.
Schmidt-Ott, K. M., Masckauchan, T. N., Chen, X., Hirsh, B. J., Sarkar, A., Yang, J., Paragas, N., Wallace, V. A., Dufort, D., Pavlidis, P. et al. (2007). beta-catenin/TCF/Lef controls a differentiation-associated transcriptional program in renal epithelial progenitors. *Development* **134**, 3177-3190.
Spilianakis, C. G. and Flavell, R. A. (2004). Long-range intrachromosomal interactions in the T helper type 2 cytokine locus. *Nat. Immunol.* **5**, 1017-1027.
Stemmler, M. P., Hecht, A., Kinzel, B. and Kemler, R. (2003). Analysis of regulatory elements of E-cadherin with reporter gene constructs in transgenic mouse embryos. *Dev. Dyn.* **227**, 238-245.
Stemmler, M. P., Hecht, A. and Kemler, R. (2005). E-cadherin intron 2 contains cis-regulatory elements essential for gene expression. *Development* **132**, 965-976.
Tao, J., Kuliyev, E., Wang, X., Li, X., Wilanowski, T., Jane, S. M., Mead, P. E. and Cunningham, J. M. (2005). BMP4-dependent expression of Xenopus Grainyhead-like 1 is essential for epidermal differentiation. *Development* **132**, 1021-1034.
Tepass, U. (2003). Claudin complexities at the apical junctional complex. *Nat. Cell Biol.* **5**, 595-597.
Tepass, U., Gruszynski-DeFeo, E., Haag, T. A., Omatyar, L., Torok, T. and Hartenstein, V. (1996). shotgun encodes Drosophila E-cadherin and is preferentially required during cell rearrangement in the neurectoderm and other morphogenetically active epithelia. *Genes Dev.* **10**, 672-685.
Ting, S. B., Wilanowski, T., Auden, A., Hall, M., Voss, A. K., Thomas, T., Parekh, V., Cunningham, J. M. and Jane, S. M. (2003). Inositol- and folate-resistant neural tube defects in mice lacking the epithelial-specific factor Grhl-3. *Nat. Med.* **9**, 1513-1519.
Ting, S. B., Caddy, J., Hislop, N., Wilanowski, T., Auden, A., Zhao, L. L., Ellis, S., Kaur, P., Uchida, Y., Holleran, W. M. et al. (2005). A homolog of Drosophila grainy head is essential for epidermal integrity in mice. *Science* **308**, 411-413.
Tinkle, C. L., Lechler, T., Pasolli, H. A. and Fuchs, E. (2004). Conditional targeting of E-cadherin in skin: insights into hyperproliferative and degenerative responses. *Proc. Natl. Acad. Sci. USA* **101**, 552-557.

Uv, A. E., Thompson, C. R. and Bray, S. J. (1994). The Drosophila tissue-specific factor Grainyhead contains novel DNA-binding and dimerization domains which are conserved in the human protein CP2. *Mol. Cell. Biol.* **14**, 4020-4031.
Venkatesan, K., McManus, H. R., Mello, C. C., Smith, T. F. and Hansen, U. (2003). Functional conservation between members of an ancient duplicated transcription factor family, LSF/Grainyhead. *Nucleic Acids Res.* **31**, 4304-4316.
Vleminckx, K. and Kemler, R. (1999). Cadherins and tissue formation: integrating adhesion and signaling. *BioEssays* **21**, 211-220.
Wang, Q. and Margolis, B. (2007). Apical junctional complexes and cell polarity. *Kidney Int.* **72**, 1448-1458.
Wilanowski, T., Tuckfield, A., Cerruti, L., O'Connell, S., Saint, R., Parekh, V., Tao, J., Cunningham, J. M. and Jane, S. M. (2002). A highly conserved novel family of mammalian developmental transcription factors related to Drosophila grainyhead. *Mech. Dev.* **114**, 37-50.
Wilanowski, T., Caddy, J., Ting, S. B., Hislop, N. R., Cerruti, L., Auden, A., Zhao, L. L., Asquith, S., Ellis, S., Sinclair, R. et al. (2008). Perturbed desmosomal cadherin expression in grainy head-like 1-null mice. *EMBO J.* **27**, 886-897.
Yang, J., Mani, S. A., Donaher, J. L., Ramaswamy, S., Itzykson, R. A., Come, C., Savagner, P., Gitelman, I., Richardson, A. and Weinberg, R. A. (2004). Twist, a master regulator of morphogenesis, plays an essential role in tumor metastasis. *Cell* **117**, 927-939.
Yu, Z., Lin, K. K., Bhandari, A., Spencer, J. A., Xu, X., Wang, N., Lu, Z., Gill, G. N., Roop, D. R., Wertz, P. et al. (2006). The Grainyhead-like epithelial transactivator Get-1/Grhl3 regulates epidermal terminal differentiation and interacts functionally with LMO4. *Dev. Biol.* **299**, 122-136.
Yu, Z., Bhandari, A., Mannik, J., Pham, T., Xu, X. and Andersen, B. (2008). Grainyhead-like factor Get1/Grhl3 regulates formation of the epidermal leading edge during eyelid closure. *Dev. Biol.* **319**, 56-67.
Yu, Z., Mannik, J., Soto, A., Lin, K. K. and Andersen, B. (2009). The epidermal differentiation-associated Grainyhead gene Get1/Grhl3 also regulates urothelial differentiation. *EMBO J.* **28**, 1890-1903.
Zhang, Y., Tomann, P., Andl, T., Gallant, N. M., Huelsken, J., Jerchow, B., Birchmeier, W., Paus, R., Piccolo, S., Mikkola, M. L. et al. (2009). Reciprocal requirements for EDA/EDAR/NF-kappaB and Wnt/beta-catenin signaling pathways in hair follicle induction. *Dev. Cell* **17**, 49-61.

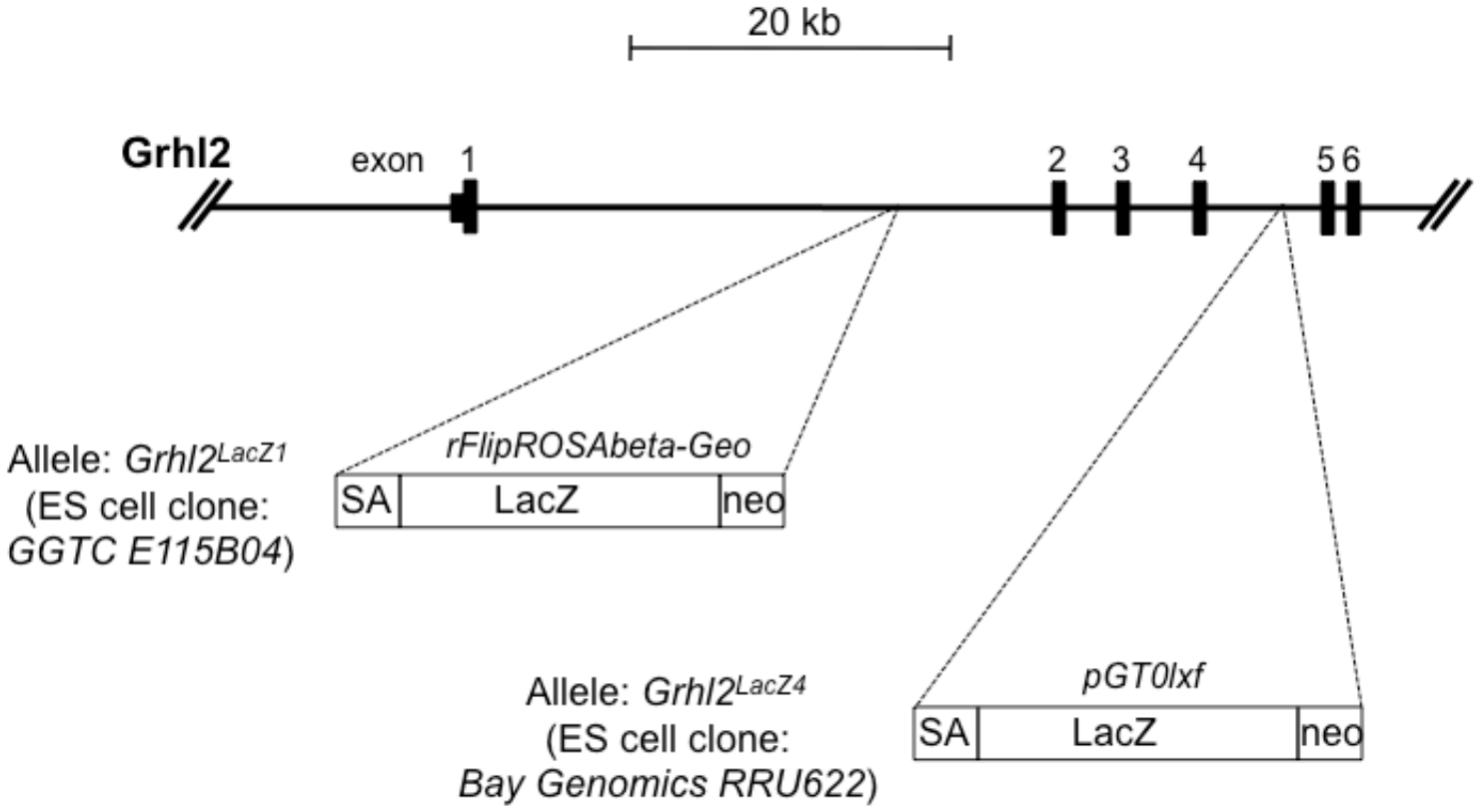
20 kb
Grhl2
exon
1
2
3
4
5
6
Allele: Grhl2LacZ1
(ES cell clone:
GGTC E115B04)
rFlipROSAbeta-Geo
SA
LacZ
neo
Allele: Grhl2LacZ4
(ES cell clone:
Bay Genomics RRU622)
pGT0lxf
SA
LacZ
neo

A

non-epithelial	epithelial	
Metanephric mesenchyme (MM)	Ureteric bud (UB) tip (T) and stalk (S)	mIMCD-3 (inner medullary collecting duct epithelia)

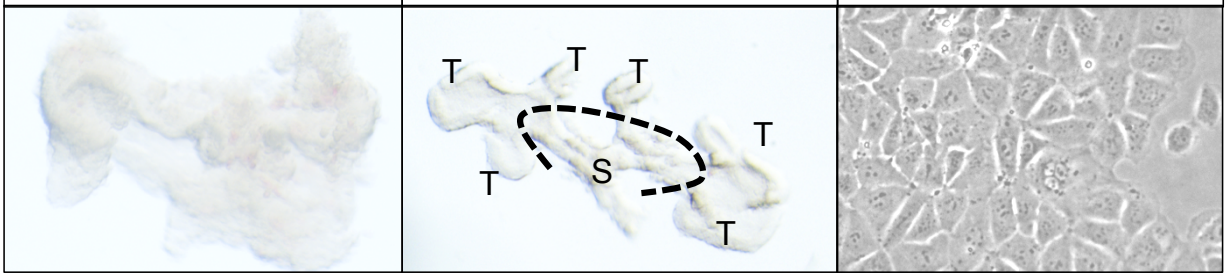

B

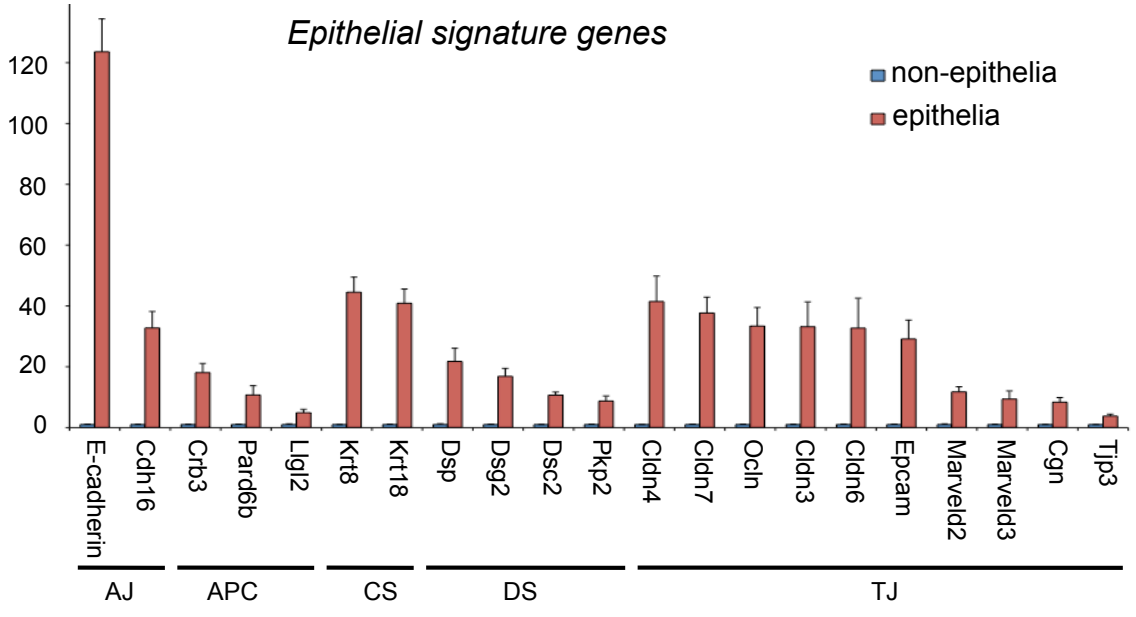

C

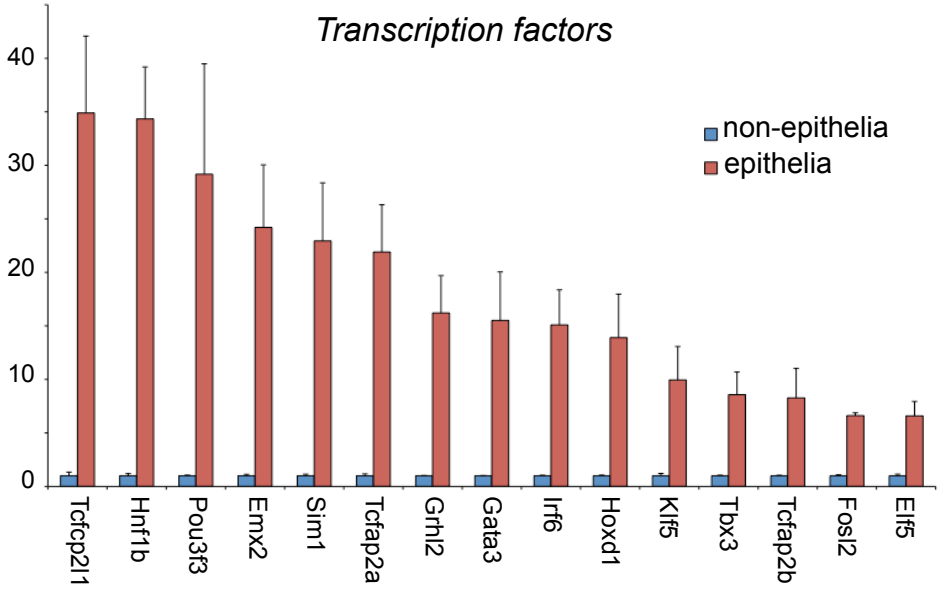

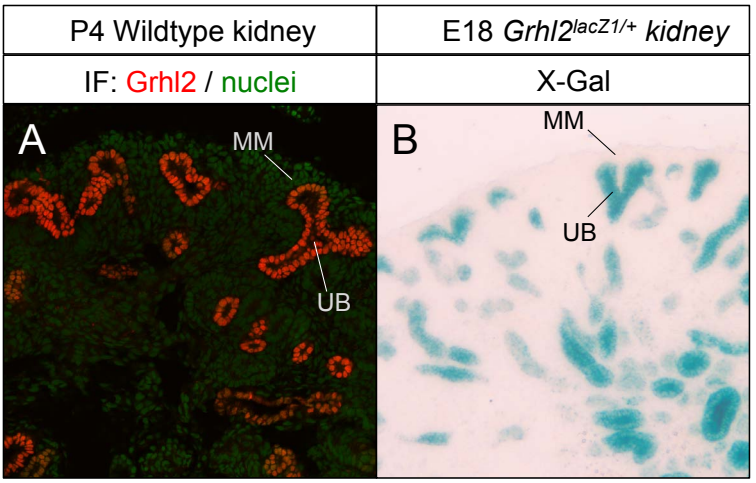
P4 Wildtype kidney
E18 Grhl2lacZ1/+ kidney
IF: Grhl2 / nuclei
X-Gal
A
MM
UB
B
MM
UB

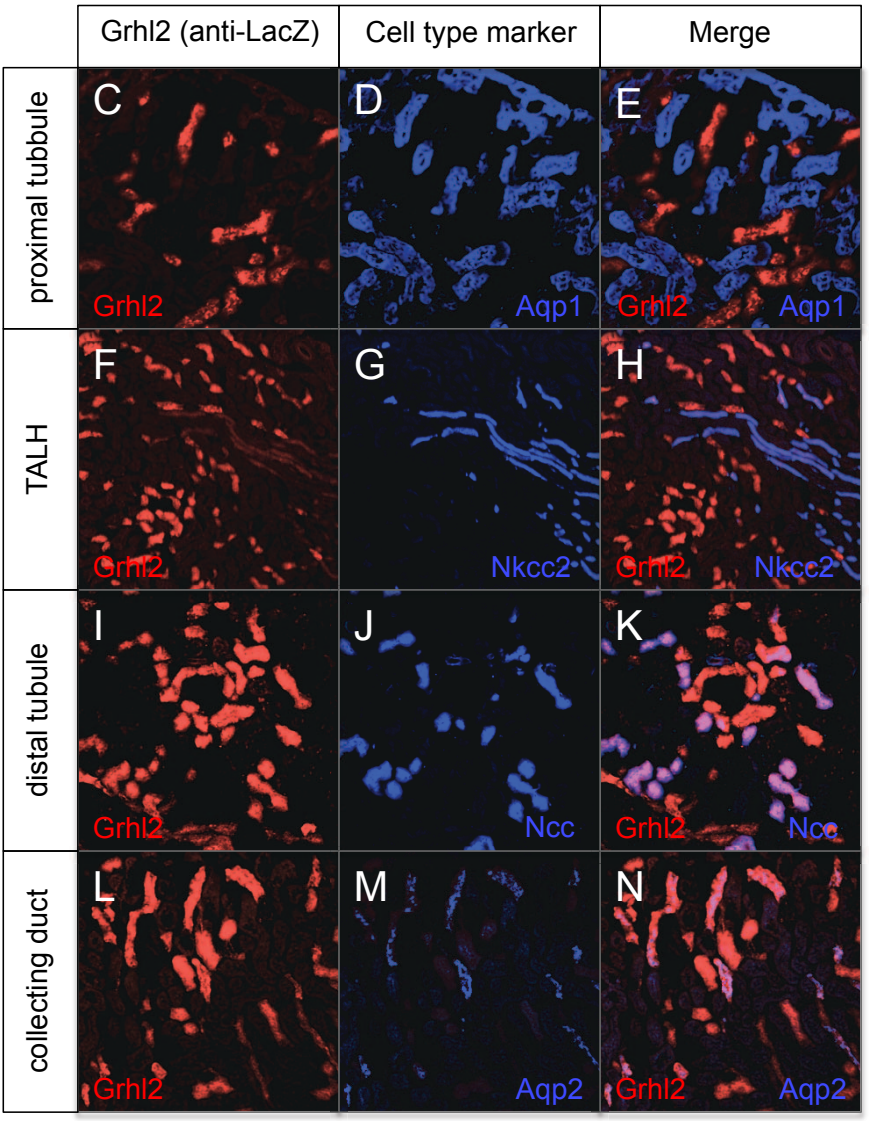
Grhl2 (anti-LacZ)
Cell type marker
Merge
proximal tubbule
TALH
distal tubule
collecting duct
C
D
E
F
G
H
I
J
K
L
M
N
Grhl2
Aqp1
Nkcc2
Ncc
Aqp2

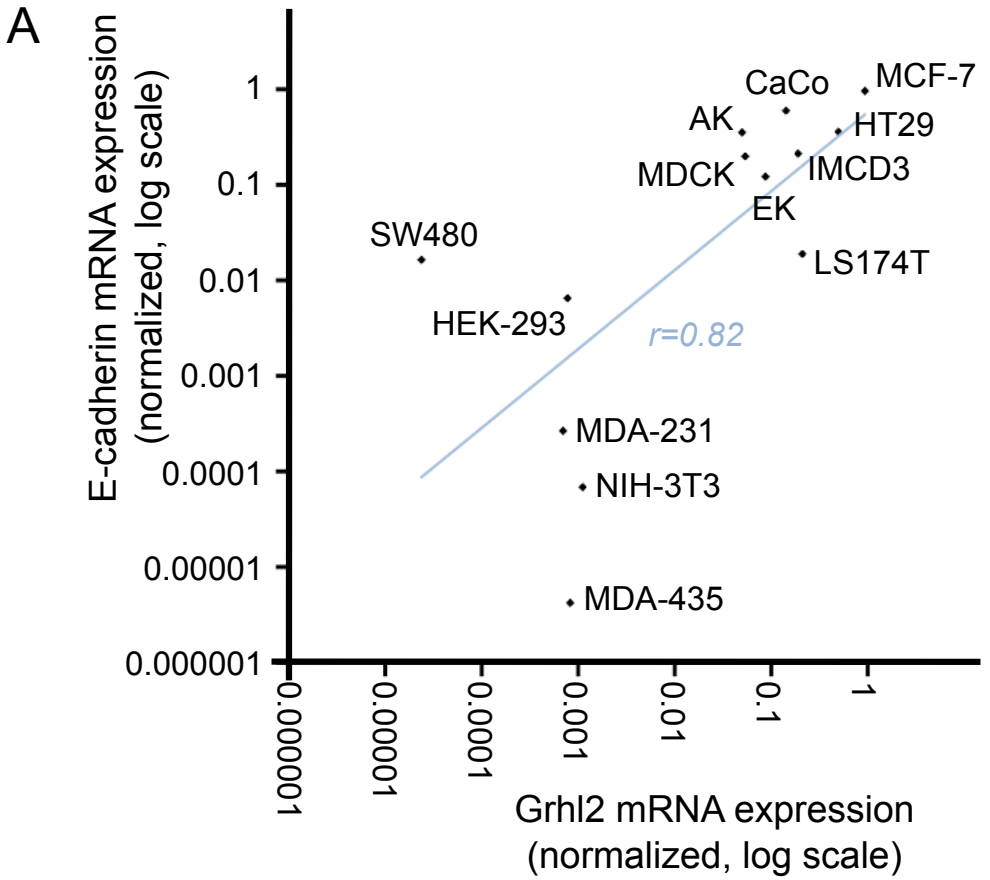
A
E-cadherin mRNA expression
(normalized, log scale)
1
0.1
0.01
0.001
0.0001
0.00001
0.000001
CaCo
MCF-7
AK
HT29
MDCK
IMCD3
EK
SW480
LS174T
HEK-293
r=0.82
MDA-231
NIH-3T3
MDA-435
0.000001
0.00001
0.0001
0.001
0.01
0.1
1
Grhl2 mRNA expression
(normalized, log scale)

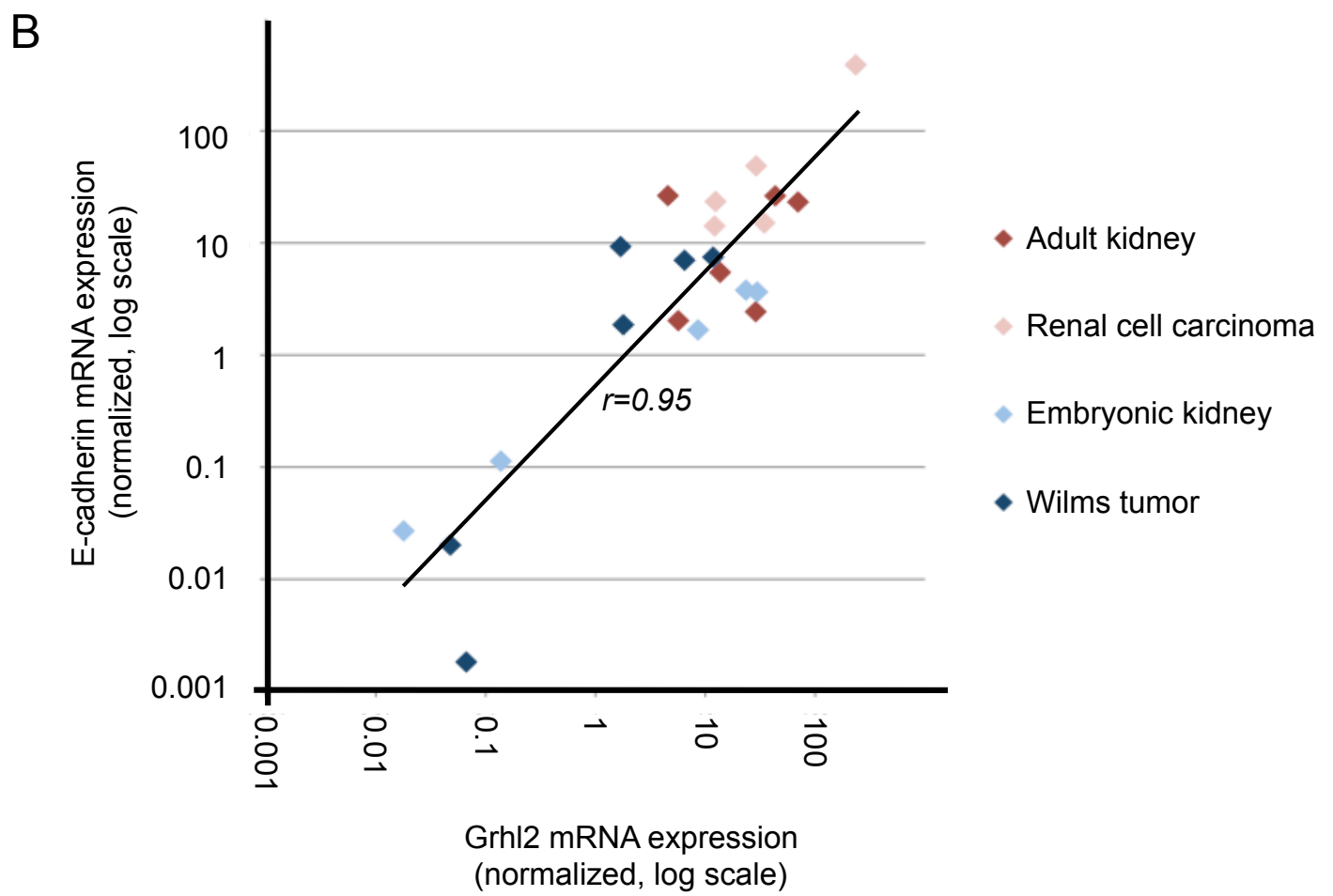
B
E-cadherin mRNA expression
(normalized, log scale)
100
10
1
0.1
0.01
0.001
r=0.95
0.001
0.01
0.1
1
10
100
Grhl2 mRNA expression
(normalized, log scale)
Adult kidney
Renal cell carcinoma
Embryonic kidney
Wilms tumor


Grhl2LacZ1/+
A
E8.0
se
gt
posterior
B
E9.5
gt
se
ov
C
E9.5
ov
pa1

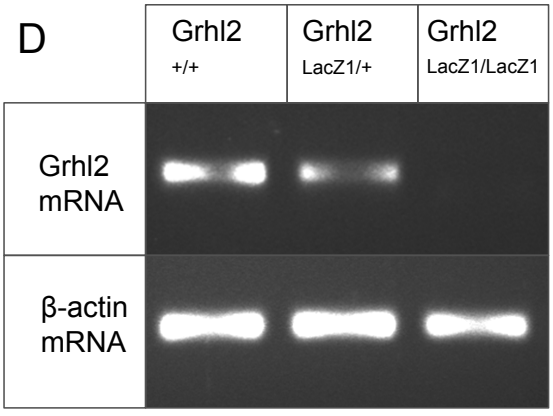
D
Grhl2 +/+
Grhl2 LacZ1/+
Grhl2 LacZ1/LacZ1
Grhl2 mRNA
β-actin mRNA

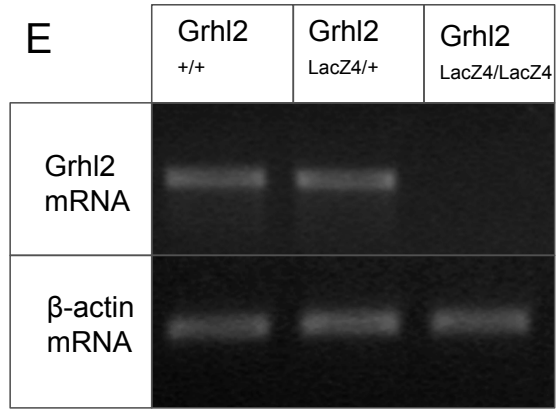
E
Grhl2 +/+
Grhl2 LacZ4/+
Grhl2 LacZ4/LacZ4
Grhl2 mRNA
β-actin mRNA

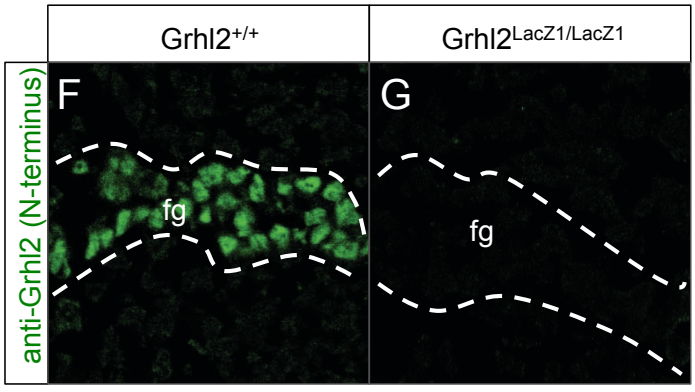
Grhl2+/+
Grhl2LacZ1/LacZ1
anti-Grhl2 (N-terminus)
F
fg
G
fg

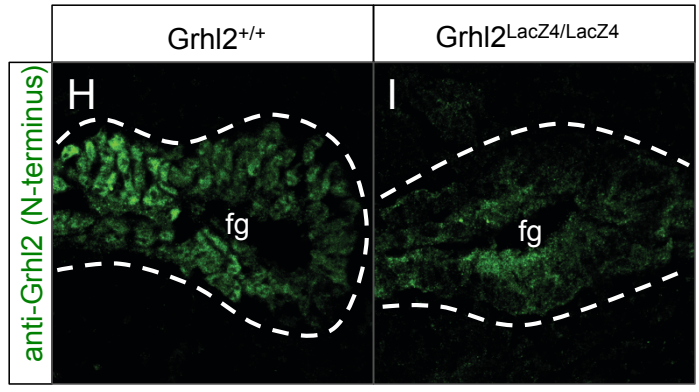
Grhl2+/+
Grhl2LacZ4/LacZ4
anti-Grhl2 (N-terminus)
H
fg
I
fg

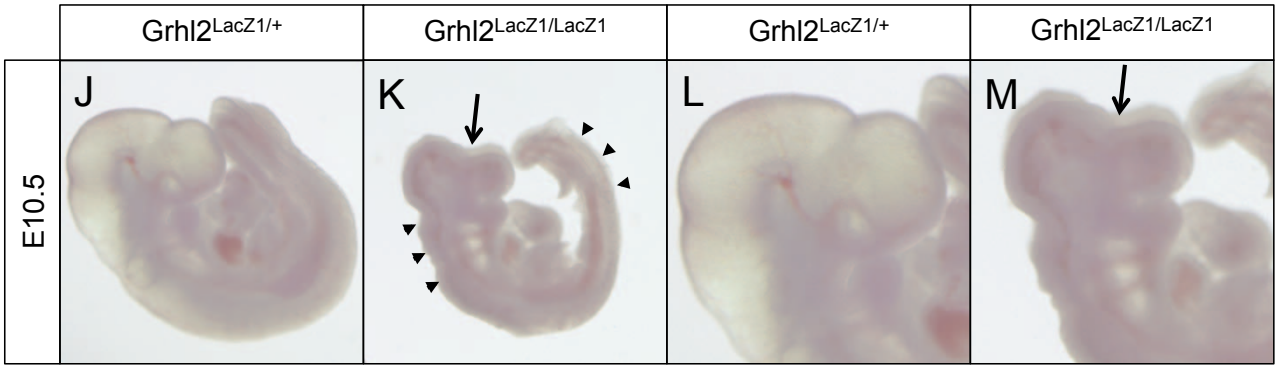
Grhl2LacZ1/+
Grhl2LacZ1/LacZ1
Grhl2LacZ1/+
Grhl2LacZ1/LacZ1
E10.5
J
K
L
M

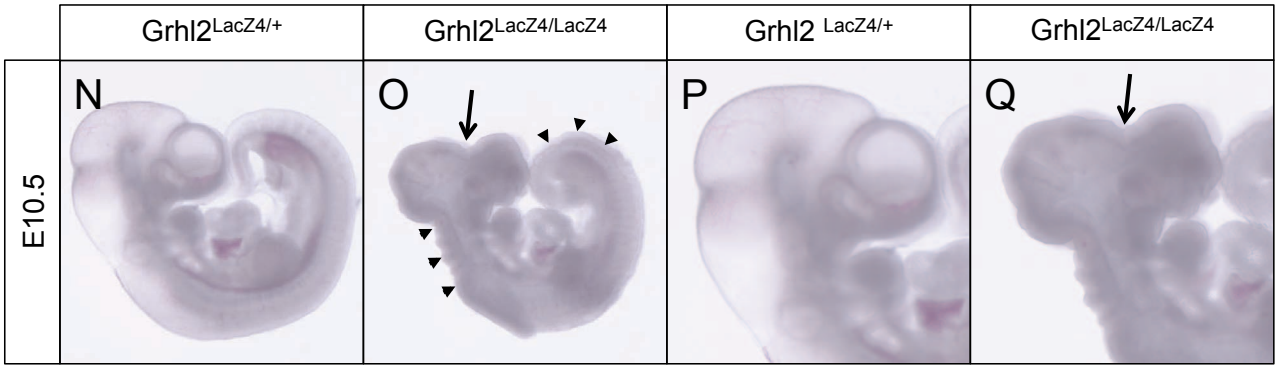
Grhl2LacZ4/+
Grhl2LacZ4/LacZ4
Grhl2 LacZ4/+
Grhl2LacZ4/LacZ4
E10.5
N
O
P
Q

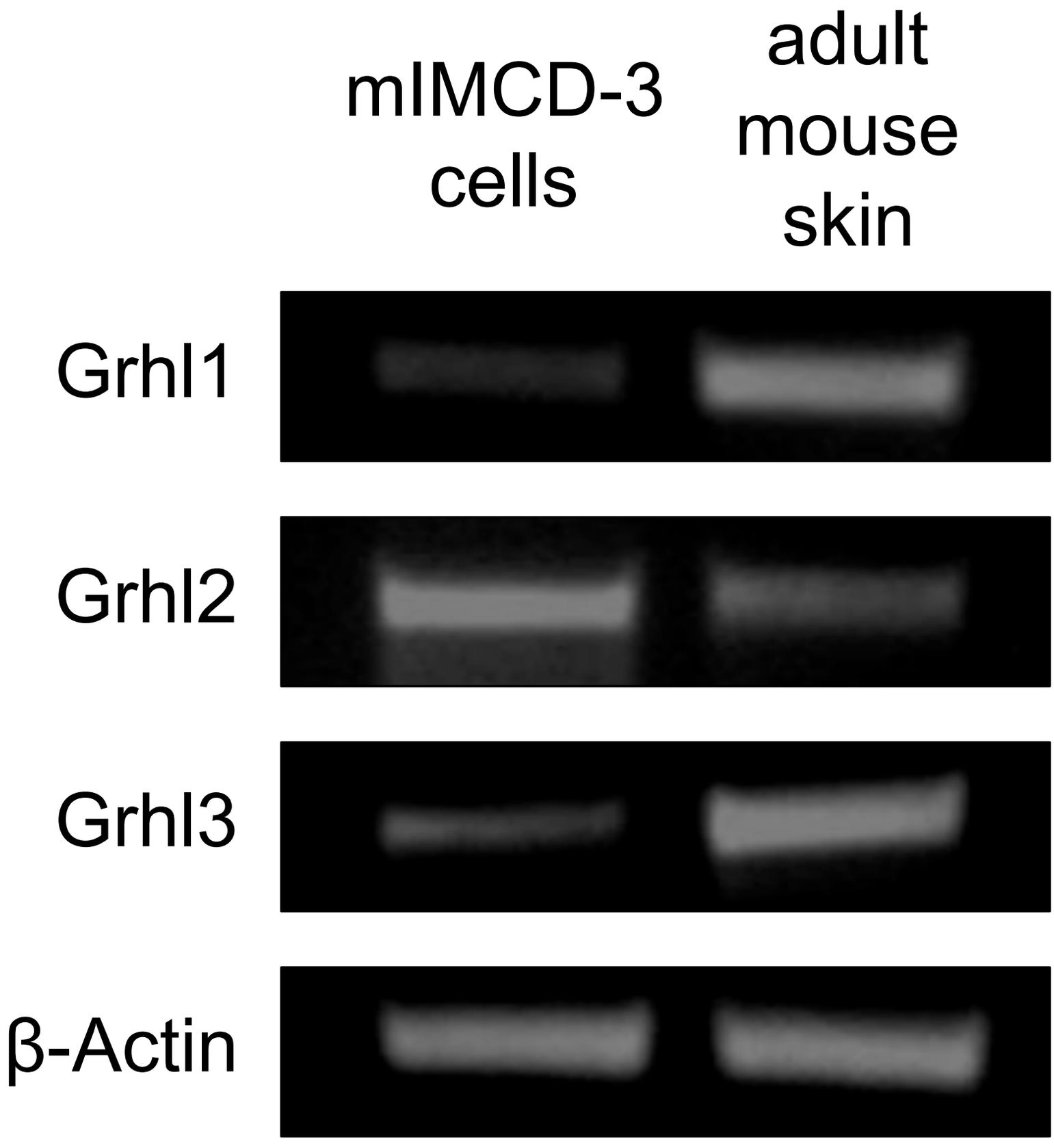
mIMCD-3 cells
adult mouse skin
Grhl1
Grhl2
Grhl3
β-Actin

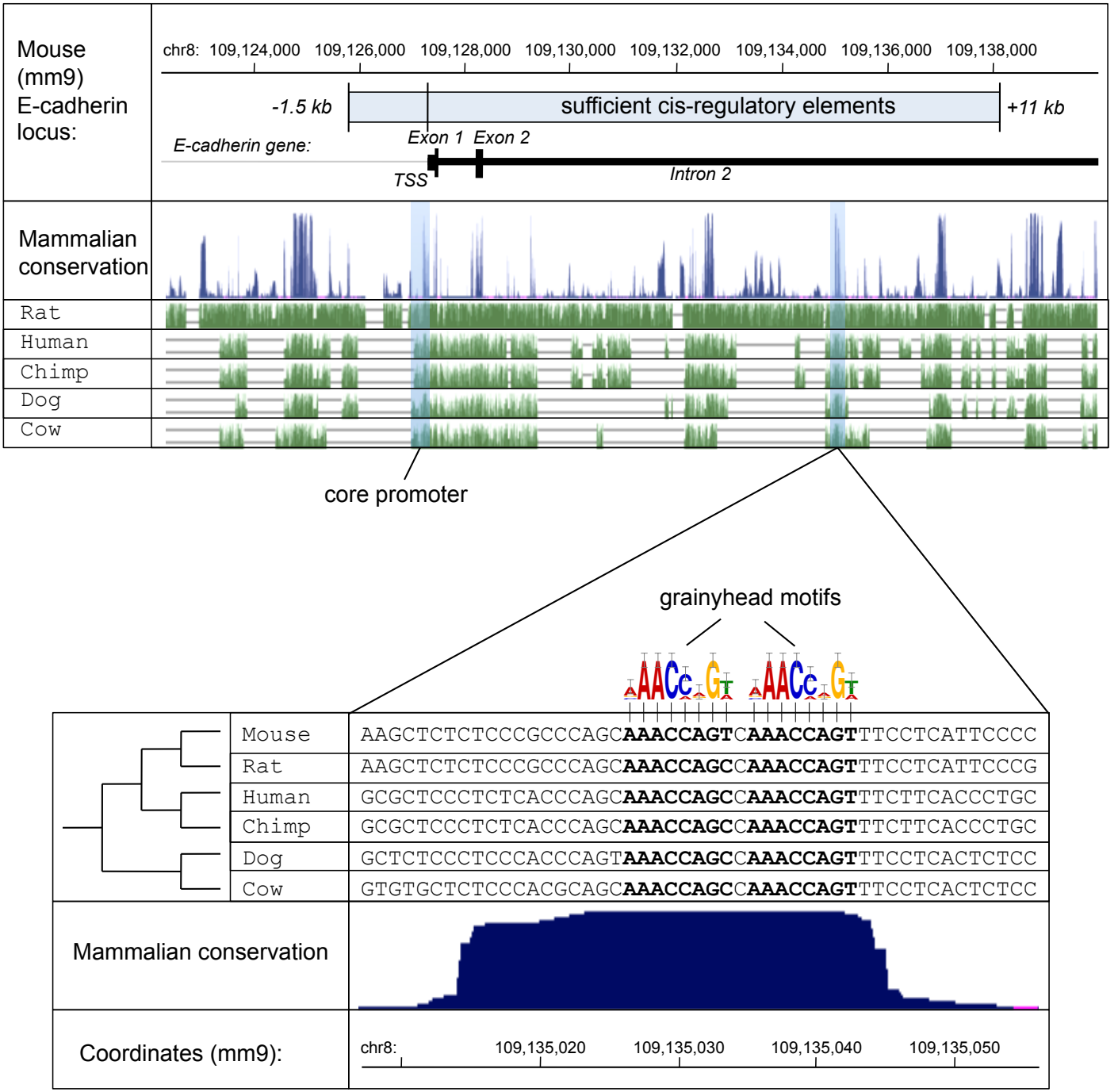
Mouse (mm9) E-cadherin locus:
chr8: 109,124,000 109,126,000 109,128,000 109,130,000 109,132,000 109,134,000 109,136,000 109,138,000
-1.5 kb
sufficient cis-regulatory elements
+11 kb
E-cadherin gene:
Exon 1 Exon 2
TSS
Intron 2
Mammalian conservation
Rat
Human
Chimp
Dog
Cow
core promoter
grainyhead motifs
Mouse AAGCTCTCTCCCGCCCAGCAAACCAGTCAAACCAGTTTCCTCATTCCCC
Rat AAGCTCTCTCCCGCCCAGCAAACCAGCCAAACCAGTTTCCTCATTCCCG
Human GCGCTCCCTCTCACCCAGCAAACCAGCCAAACCAGTTTCTTCACCCTGC
Chimp GCGCTCCCTCTCACCCAGCAAACCAGCCAAACCAGTTTCTTCACCCTGC
Dog GCTCTCCCTCCCACCCAGTAAACCAGCCAAACCAGTTTCCTCACTCTCC
Cow GTGTGCTCTCCCACGCAGCAAACCAGCCAAACCAGTTTCCTCACTCTCC
Mammalian conservation
Coordinates (mm9):
chr8: 109,135,020 109,135,030 109,135,040 109,135,050

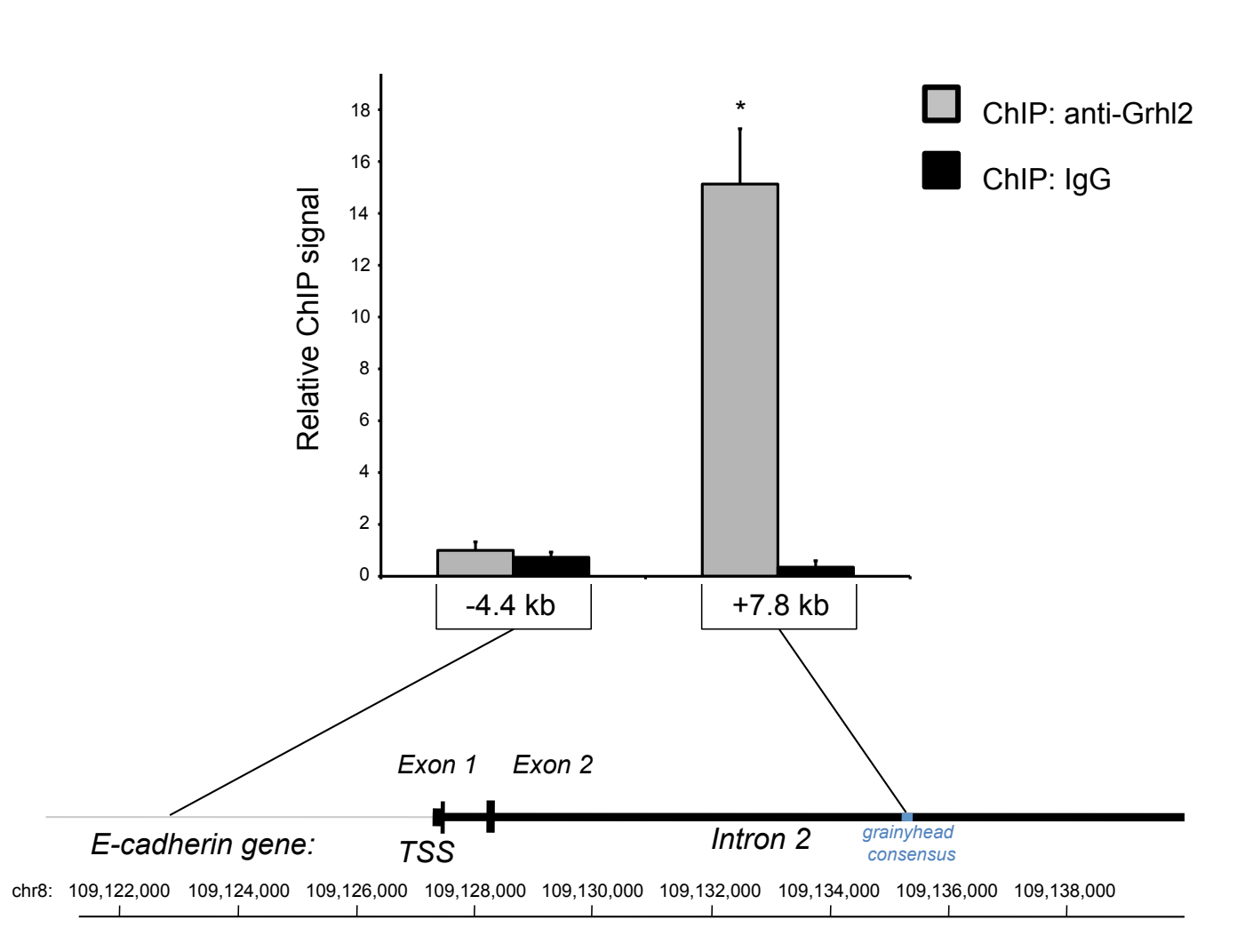
ChIP: anti-Grhl2
ChIP: IgG
Relative ChIP signal
18
16
14
12
10
8
6
4
2
0
*
-4.4 kb
+7.8 kb
Exon 1
Exon 2
E-cadherin gene:
TSS
Intron 2
grainyhead
consensus
chr8:
109,122,000
109,124,000
109,126,000
109,128,000
109,130,000
109,132,000
109,134,000
109,136,000
109,138,000

A

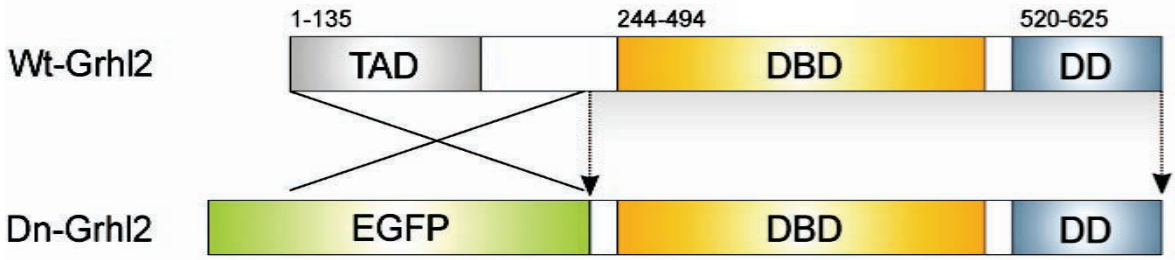
1-135
244-494
520-625
Wt-Grhl2
TAD
DBD
DD
Dn-Grhl2
EGFP
DBD
DD

B

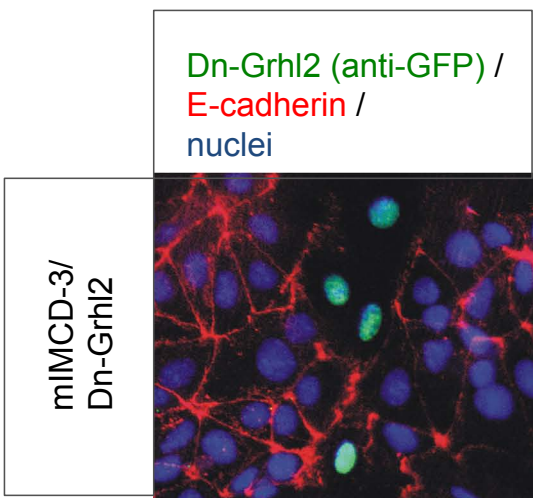
Dn-Grhl2 (anti-GFP) /
E-cadherin /
nuclei
mIMCD-3/
Dn-Grhl2

C

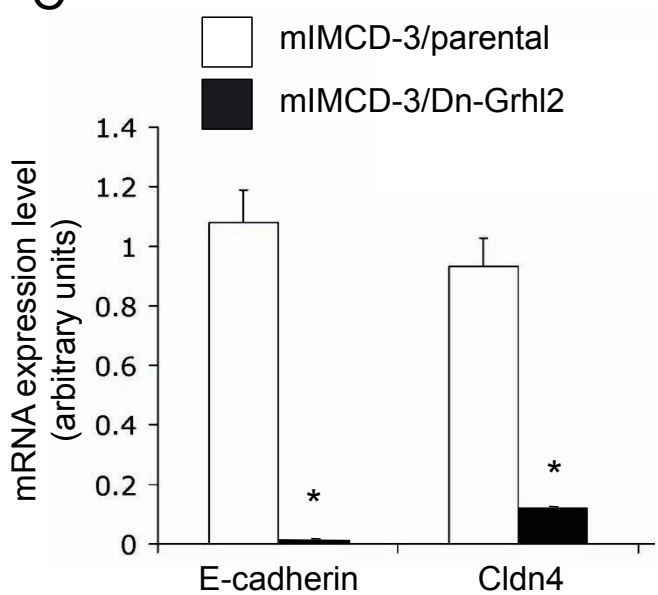
mIMCD-3/parental
mIMCD-3/Dn-Grhl2
mRNA expression level
(arbitrary units)
1.4
1.2
1
0.8
0.6
0.4
0.2
0
*
*
E-cadherin
Cldn4

D

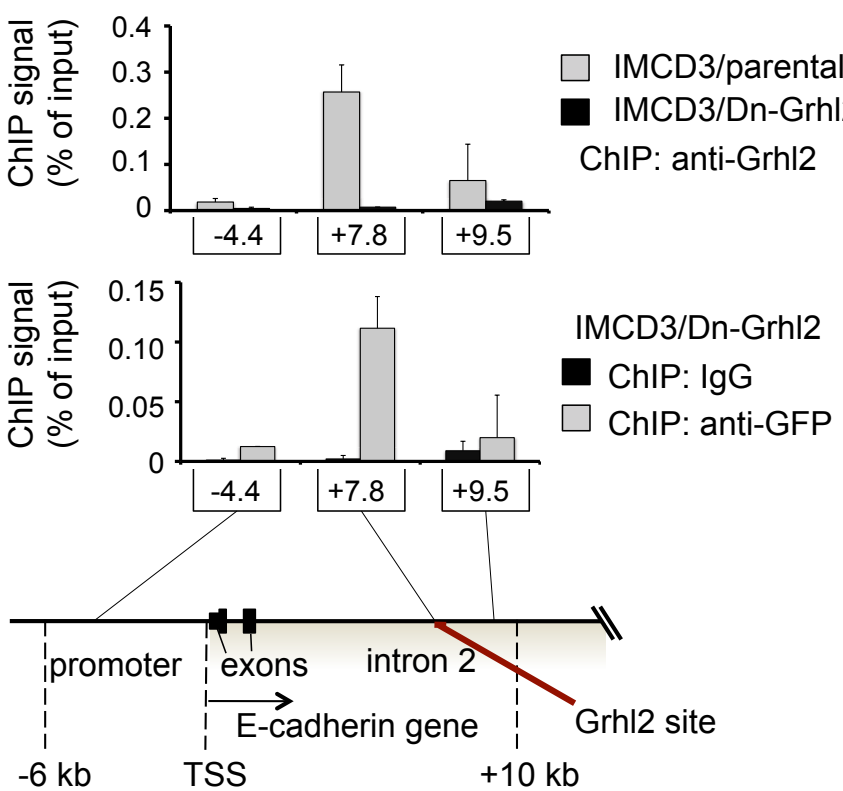
ChIP signal
(% of input)
0.4
0.3
0.2
0.1
0
-4.4
+7.8
+9.5
IMCD3/parental
IMCD3/Dn-Grhl2
ChIP: anti-Grhl2
ChIP signal
(% of input)
0.15
0.10
0.05
0
-4.4
+7.8
+9.5
IMCD3/Dn-Grhl2
ChIP: IgG
ChIP: anti-GFP
promoter
exons
intron 2
E-cadherin gene
Grhl2 site
-6 kb
TSS
+10 kb

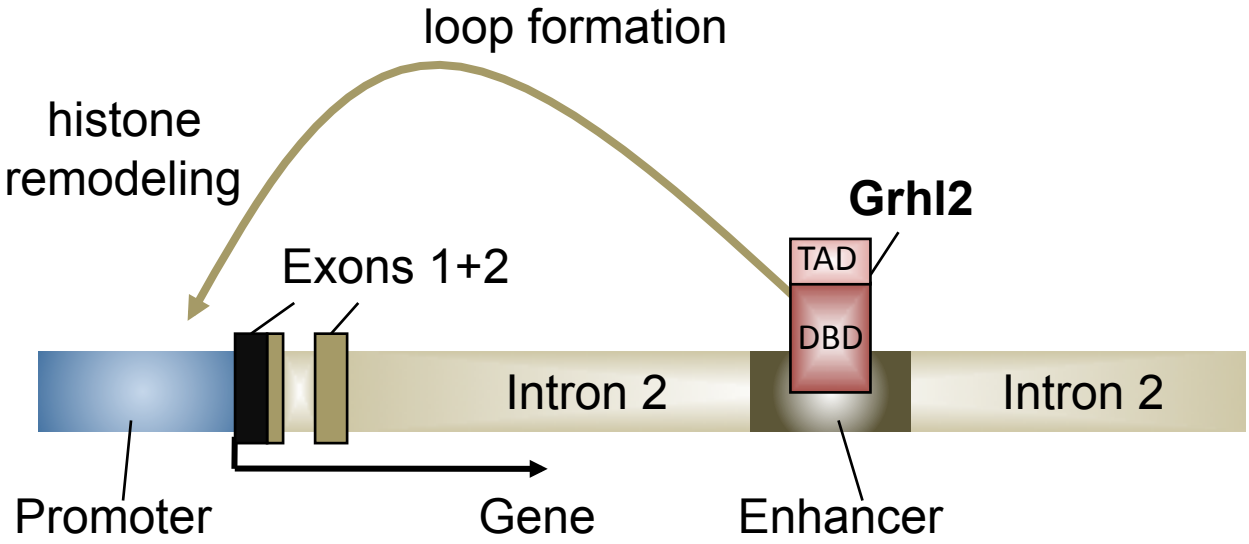

E-cadherin locus

Table S1. Oligonucleotide sequences

ChiP primers for E-Cadherin locus

Position, in kb relative to E-cadherin TSS	Forward primer sequence	Reverse primer sequence
–4.4	AGGAGGATTGCCCTGAAAGT	GAGAGACGGAGAAGGAACAA
–2.6	AAGAAAGCAACGCTCCAAAG	AGGGCGAGGACTCTGGTATT
–0.1	CGCACTACTGAGTTCCCAAG	GTCAGGACCCTCCACATACC
1.7	AAGGCAAGAGGACCAGGTTT	CCCAGAAAGGGATTGTGTGT
3.6	AACCGAGGATTGTGACCTTG	GGATATGCTTGGGTAGTGGA
7.8 (primer pair A)	GAAGCCTTTCCCTTTCCATT	ACCCTTTCTAAGGCACAGCA
7.8 (primer pair B)	CAGCAAACCAGTCAAACCAG	TTTCTAAGGCACAGCAAACC
9.5	AGGTGGGAAGGAAACCAGTC	CAGGTTCATCTTCAGGCACA

ChiP primers for *Cldn4* locus

Position, in kb relative to Cldn4 TSS	Forward primer sequence	Reverse primer sequence
–0.1	GTGATACTGGCGGGTGACTC	GGGACCAGTTTCTCTGGATTC
2.8	ACAGGGAAGGGTTCTGTGTG	GGGTCTTGTATCCTGGCTGA

Real-time RT-PCR primers

Gene	Forward primer sequence	Reverse primer sequence
β-Actin (mouse, rat, human, dog)	TTCAACACCCCAGCCATGTA	GTGGTGGTGAAGCTGTAGCC
Grhl1 (mouse)	AAATTCGGGATGAAGAACGA	TCAGCTTAGCAGGAGGAGGA
Grhl2 (mouse, rat, human, dog)	CAAAGCAAGTGACAGCCAAG	CTTTGTTGAGGTAGGTCATGG
Grhl2 (mouse)	ACCATCGGGAACATTGAAGA	TCCGGTCCTCTGTAGGTTTG
Grhl3 (mouse)	GCCTACCTCAACAAGGGTCA	TGCCTGCTCCACAGTCATAG
E-cadherin (mouse, rat, human, dog)	AAGGGCTTGGATTTTGAGG	AGATGGGGGCTTCATTCAC
E-cadherin (mouse)	CGTCCATGTGTGTGACTGTG	GGAGCCACATCATTTCGAGT
Cldn4 (mouse)	GGCGTCTATGGGACTACAGG	GGTTGTAGAAGTCGCGGATG

Primers used for genotyping

DNA fragment	Forward primer sequence	Reverse primer sequence
Grhl2-LacZ1 mutant allele (500 bp)	AAAGGCATCAAGGTGTGAGC	GTGCGCATAGTGGCTTGAAT
Grhl2-LacZ1 wildtype allele (621 bp)	CACGTAGACGAGCTCTGTGG	GTGGGCAGTTGGTGTTTGAG
Grhl2-LacZ4 mutant allele (261 bp)	TGCATGCTGAACTCTGGAGGTGGTG	ACTTCCGGAGCGATCTCAAACTCTC
Grhl2-LacZ4 wildtype allele (396 bp)	TGCATGCTGAACTCTGGAGGTGGTG	ACAGCTCAGCACATGAAGCATCAGATG

Primers for production of riboprobes

Gene	Forward primer sequence	Reverse primer sequence (including T7 promoter sequences)
E-cadherin	ATCGCCTACACCATCGTCAG	GGCCAGTGAATTGTAATACGACTCACTATAGGG AGGCGGTATGAGGCTGTGGGTTCCTC
Cldn4	TGCTTCTCTCAGTGGTAGGG	GGCCAGTGAATTGTAATACGACTCACTATAGGG AGGCGGTAAGGAGCCATGTGGA

Primers for 3C assay

Primer	Primer sequence	Distance from *Bgl*II site
Control reverse (cr)	ATTCTCTCTTTTCCGCCATATGTA	124 bp
Promoter reverse (pr)	TTTGTTTTGTTGTTGTTGCTTTTTA	86 bp
Enhancer reverse (er)	AGAGTGGTGAATCCCTGTATATCAA	50 bp

Oligos for Splinkerette (SPLK) PCR

Oligo	Oligo sequence
SPLK adaptor A	CGAAGAGTAACCGTTGCTAGGAGAGACCGTGGCTGAATGAGACTGGTGTCGACACTAGTGG
SPLK adaptor B	GATCCCACTAGTGTCGACACCAGTCTCTAATTTTTTTTTTCAAAAAAA
SPLK forward primer outer	CGAAGAGTAACCGTTGCTAGGAGAGACC
SPLK reverse primer outer	GCTCTGTCCTCCAGTCTCCTCCAC
SPLK forward primer nested	GTGGCTGAATGAGACTGGTGTCGAC
SPLK reverse primer nested	ACACACTCCAACCTCCGCAAACTC